November, the 9th, 2020

A port-Hamiltonian formulation of flexible structures
Modelling and structure preserving finite element discretization

Andrea Brugnoli

Supervisors

Thesis director: Daniel Alazard

Co-director: Valérie Pommier-Budinger

Co-supervisor: Denis Matignon

INFIDHEM

Institut Supérieur de l'Aéronautique et de l'Espace

Outline

Outline

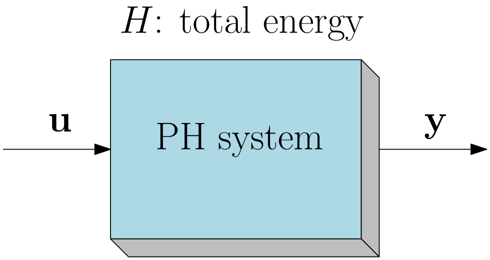

Lossless: $\dot{H} = \mathbf{u}^\top \mathbf{y}$

Passive: $\dot{H} \leq \mathbf{u}^\top \mathbf{y}$

PH systems are:

- Physically motivated;
- Lumped (ODEs) or distributed (PDEs);
- Passive (passivity based control);
- Closed under interconnection (modular multiphysics modelling);

Why port-Hamiltonian systems?

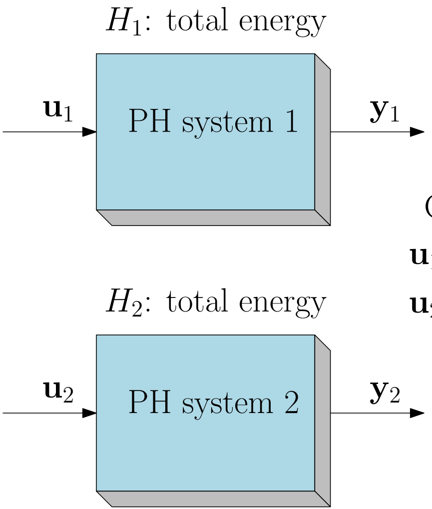

Gyrator

$$\mathbf{u}_1 = -\mathbf{y}_2$$
$$\mathbf{u}_2 = +\mathbf{y}_1$$

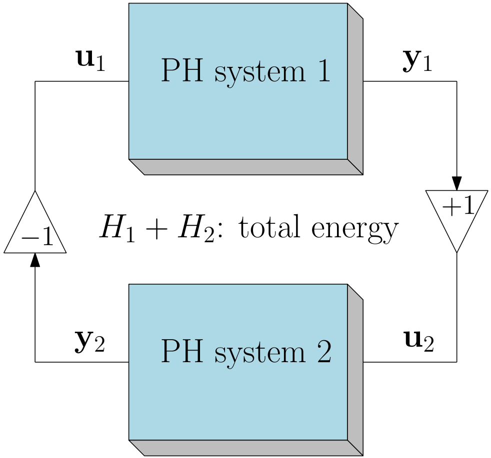

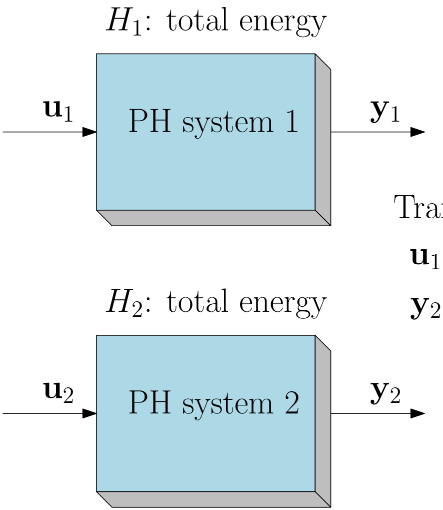

Transformer

$$\mathbf{u}_1 = -\mathbf{u}_2$$

$$\mathbf{y}_2 = +\mathbf{y}_1$$

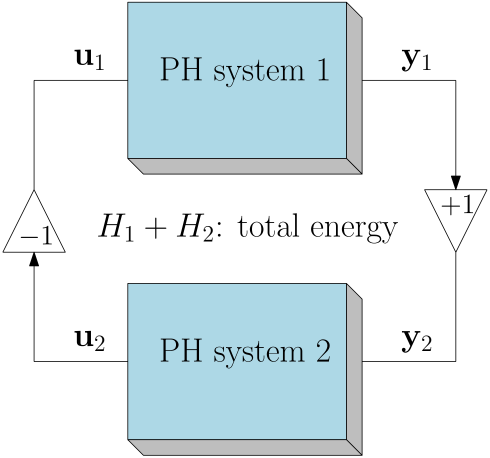

They have been used for simulating and controlling a variety of applications[1]:

- flexible thin beams;
- acoustic waves;
- stirred tank reactors;
- plasma in tokamak;
- shallow water equations;
- fluid-structure interactions.

Distributed port-Hamiltonian systems

$\partial_t \boldsymbol{\alpha} = \mathcal{J}\, \boldsymbol{e}$,	$\boldsymbol{\alpha}$	Energy variables,	$\mathcal{J}$	Skew-symmetric operator,
$\boldsymbol{e} := \delta_{\boldsymbol{\alpha}} H$,	$\boldsymbol{e}$	Co-energy variables,		
$\boldsymbol{u}_\partial = \mathcal{B}_\partial\, \boldsymbol{e}$,	$\boldsymbol{u}_\partial$	Control input,	$\mathcal{B}_\partial$	Input operator,
$\boldsymbol{y}_\partial = \mathcal{C}_\partial\, \boldsymbol{e}$,	$\boldsymbol{y}_\partial$	Control output.	$\mathcal{C}_\partial$	Output operator.

[1] R. Rashad et al. “Twenty years of distributed port-Hamiltonian systems: a literature review”. In: *IMA Journal of Mathematical Control and Information* (July 2020).

Motivation & Research Objectives

A missing piece in the port-Hamiltonian literature

Despite all the preexisting literature, models arising from structural mechanics on multidimensional geometrical domains have rarely been considered[2].

Purpose of this work

This thesis aims to establish a consistent pH formulation of flexible structures, together with a symplectic discretization method.

Methodologies

The numerical implementation relies on efficient and well-established libraries, to avoid constructing everything from scratch.

[2] A. Macchelli, C. Melchiorri, and L. Bassi. "Port-based Modelling and Control of the Mindlin Plate". In: *Proceedings of the 44th IEEE Conference on Decision and Control*. 2005, pp. 5989–5994.

Flexible systems pH modelling:

- Mindlin plate: Stokes-Dirac formulation[3], jet bundle formalism[4];
- Kirchhoff plate: jet bundle formalism[5].

This contribution

Stokes-Dirac formulation of linear elastodynamics and plate models.

[3] A. Macchelli, C. Melchiorri, and L. Bassi. "Port-based Modelling and Control of the Mindlin Plate". In: *Proceedings of the 44th IEEE Conference on Decision and Control*. 2005, pp. 5989–5994.

[4] M. Schöberl and K. Schlacher. "Variational Principles for Different Representations of Lagrangian and Hamiltonian Systems". In: *Dynamics and Control of Advanced Structures and Machines*. Ed. by Hans Irschik, Alexander Belyaev, and Michael Krommer. Springer International Publishing, 2017, pp. 65–73.

[5] M. Schöberl and K. Schlacher. "On the extraction of the boundary conditions and the boundary ports in second-order field theories". In: *Journal of Mathematical Physics* 59.10 (2018), p. 102902.

Discretization of port-Hamiltonian systems:

- Mixed finite elements for differential forms[6];
- Spectral methods[7];
- Finite differences[8].

This contribution

Mixed finite element for PDEs, applicable to generic hyperbolic and parabolic systems under uniform or mixed boundary conditions. Conjectured error estimates for linear flexible structures.

---

[6] G. Golo et al. "Hamiltonian discretization of boundary control systems". In: *Automatica* 40.5 (2004), pp. 757–771, P. Kotyczka, B. Maschke, and L. Lefèvre. "Weak form of Stokes-Dirac structures and geometric discretization of port-Hamiltonian systems". In: *Journal of Computational Physics* 361 (2018), pp. 442 –476.

[7] R. Moulla, L. Lefevre, and B. Maschke. "Pseudo-spectral methods for the spatial symplectic reduction of open systems of conservation laws". In: *Journal of computational Physics* 231.4 (2012), pp. 1272–1292.

[8] V. Trenchant et al. "Finite differences on staggered grids preserving the port-Hamiltonian structure with application to an acoustic duct". In: *Journal of Computational Physics* 373 (June 2018).

Modular modelling of flexible multibody systems:

- Model for a flexible link under large deformations using Lie algebra and differential forms[9];
- Construction of complex multibody (under large deformation) using oriented graphs[10];
- Linear modelling of structural dynamics in pH form[11].

This contribution

A pH model of floating flexible structure under small deformations (floating frame of reference approach). The paradigm includes all linear models detailed in the thesis.

[9] A. Macchelli, C. Melchiorri, and S. Stramigioli. "Port-Based Modeling of a Flexible Link". In: *IEEE Transactions on Robotics* 23 (2007), pp. 650 –660.

[10] A. Macchelli, C. Melchiorri, and S. Stramigioli. "Port-Based Modeling and Simulation of Mechanical Systems With Rigid and Flexible Links". In: *IEEE Transactions on Robotics* 25.5 (2009), pp. 1016–1029.

[11] A. Warsewa et al. "A port-Hamiltonian approach to modeling the structural dynamics of complex systems". In: *Applied Mathematical Modelling* 89 (2020), pp. 1528–1546.

Outline

Main steps for the derivation

The derivation of the Hamiltonian system relies on few simple steps to define:

1. the total energy, the energy and co-energy variables;
2. the resulting dynamics $\mathcal{J}$;
3. the boundary variables (energy rate and the Stokes theorem).

The construction is exactly the same for plate models, as they represent particular instances of this problem.

The Linear Elastodynamics problem

For small deformations, the displacement $\boldsymbol{u}$ within a continuum satisfies the PDE

$$\rho \frac{\partial^2 \boldsymbol{u}}{\partial t^2} - \mathrm{Div}(\boldsymbol{\mathcal{D}}\, \mathrm{Grad}\, \boldsymbol{u}) = 0, \qquad \boldsymbol{x} \in \Omega \subset \mathbb{R}^d,\ d \in \{2, 3\}.$$

Parameters:

- ρ mass density;
- $\boldsymbol{\mathcal{D}}(\cdot) := \frac{E}{1+\nu}\left[(\cdot) + \frac{\nu}{1-2\nu}\mathrm{Tr}(\cdot)\boldsymbol{I}\right]$ the stiffness tensor (symmetric and positive).

Stress and strain tensors:

- $\boldsymbol{\varepsilon} := \mathrm{Grad}\, \boldsymbol{u}$ the strain tensor (symmetric);
- $\boldsymbol{\Sigma} := \boldsymbol{\mathcal{D}}\boldsymbol{\varepsilon}$ the stress tensor (symmetric).

Operators:

- $\mathrm{Grad}\, \boldsymbol{u} := \frac{1}{2}\left[\nabla \boldsymbol{u} + \nabla^\top \boldsymbol{u}\right]$ the symmetric gradient;
- $\mathrm{Div}\, \boldsymbol{\Sigma} := \left(\sum_{i=1}^{d} \frac{\partial \Sigma_{ij}}{\partial x_i}\right)_{1 \leq j \leq d}$ the tensor divergence.

Energy and co-energy variables

Total energy

$$H = \frac{1}{2}\int_\Omega \left\{\rho \left\|\partial_t \boldsymbol{u}\right\|^2 + \boldsymbol{\Sigma} : \boldsymbol{\varepsilon}\right\} \, \mathrm{d}\Omega, \qquad \boldsymbol{A} : \boldsymbol{B} = \mathrm{Tr}(\boldsymbol{A}^\top \boldsymbol{B}) \quad \text{Tensor contraction.}$$

Energy variables

$$\boldsymbol{\alpha}_v = \rho \partial_t \boldsymbol{u}, \quad \text{Linear momentum,} \qquad \boldsymbol{A}_\varepsilon = \boldsymbol{\varepsilon}, \quad \text{Strain tensor.}$$

Co-energy variables

$$\boldsymbol{e}_v = \frac{\delta H}{\delta \boldsymbol{\alpha}_v} = \partial_t \boldsymbol{u}, \quad \text{Linear velocity,} \qquad \boldsymbol{E}_\varepsilon = \frac{\delta H}{\delta \boldsymbol{A}_\varepsilon} = \boldsymbol{\mathcal{D}} \boldsymbol{A}_\varepsilon = \boldsymbol{\Sigma}, \quad \text{Stress tensor.}$$

Interconnection operator and boundary variables

Dynamics

$$\frac{\partial}{\partial t}\begin{pmatrix}\boldsymbol{\alpha}_v \\ \boldsymbol{A}_\varepsilon\end{pmatrix} = \underbrace{\begin{bmatrix}\boldsymbol{0} & \mathrm{Div} \\ \mathrm{Grad} & \boldsymbol{0}\end{bmatrix}}_{\mathcal{J}}\begin{pmatrix}\boldsymbol{e}_v \\ \boldsymbol{E}_\varepsilon\end{pmatrix}.$$

Theorem

The formal adjoint of the $-\mathrm{Div}$ operator is the symmetric gradient Grad.

Hence $\mathcal{J}$ is skew-symmetric.

Boundary variables

$$\begin{aligned}\dot{H} &= \int_\Omega \{\boldsymbol{e}_v \cdot \mathrm{Div}\, \boldsymbol{E}_\varepsilon + \boldsymbol{E}_\varepsilon : \mathrm{Grad}\, \boldsymbol{e}_v\}\, \mathrm{d}\Omega, && \text{Stokes theorem,} \\ &= \int_{\partial\Omega} \boldsymbol{e}_v \cdot (\boldsymbol{E}_\varepsilon \boldsymbol{n})\, \mathrm{d}S = \langle \gamma_0 \boldsymbol{e}_v, \gamma_n \boldsymbol{E}_\varepsilon \rangle_{\partial\Omega}.\end{aligned}$$

- $\gamma_0 \boldsymbol{e}_v = \boldsymbol{e}_v|_{\partial\Omega}$ the Dirichlet trace of the velocity;
- $\gamma_n \boldsymbol{E}_\varepsilon = \boldsymbol{E}_\varepsilon \boldsymbol{n}|_{\partial\Omega}$ the normal trace of the stress tensor.

The port-Hamiltonian formulation

Given the fact that mixed boundary conditions are considered, the trace operators are restricted to the boundary partitions:

- $\gamma_0^{\Gamma_*}$ denotes the Dirichlet trace over the set Γ_*, $\gamma_0^{\Gamma_*}\boldsymbol{e}_v = \boldsymbol{e}_v|_{\Gamma_*}$;
- $\gamma_n^{\Gamma_*}$ denotes the normal trace over the set Γ_*, $\boldsymbol{\gamma}_{\boldsymbol{n}}^{\Gamma_*}\boldsymbol{E}_\varepsilon = \boldsymbol{E}_\varepsilon\boldsymbol{n}|_{\Gamma_*}$.

PH linear elasticity

$$\frac{\partial}{\partial t}\begin{pmatrix}\boldsymbol{\alpha}_v \\ \boldsymbol{A}_\varepsilon\end{pmatrix} = \underbrace{\begin{bmatrix}\mathbf{0} & \mathrm{Div} \\ \mathrm{Grad} & \mathbf{0}\end{bmatrix}}_{\mathcal{J}}\begin{pmatrix}\boldsymbol{e}_v \\ \boldsymbol{E}_\varepsilon\end{pmatrix}, \qquad \begin{pmatrix}\boldsymbol{e}_v \\ \boldsymbol{E}_\varepsilon\end{pmatrix} = \underbrace{\begin{bmatrix}\frac{1}{\rho} & \mathbf{0} \\ \mathbf{0} & \boldsymbol{\mathcal{D}}\end{bmatrix}}_{\mathcal{Q}}\begin{pmatrix}\boldsymbol{\alpha}_v \\ \boldsymbol{A}_\varepsilon\end{pmatrix},$$

$$\boldsymbol{u}_\partial = \underbrace{\begin{bmatrix}{\color{blue}\gamma_0^{\Gamma_D}} & \mathbf{0} \\ \mathbf{0} & {\color{red}\boldsymbol{\gamma}_{\boldsymbol{n}}^{\Gamma_N}}\end{bmatrix}}_{\mathcal{B}_\partial}\begin{pmatrix}\boldsymbol{e}_v \\ \boldsymbol{E}_\varepsilon\end{pmatrix}, \qquad \boldsymbol{y}_\partial = \underbrace{\begin{bmatrix}\mathbf{0} & {\color{blue}\boldsymbol{\gamma}_{\boldsymbol{n}}^{\Gamma_D}} \\ {\color{red}\gamma_0^{\Gamma_N}} & \mathbf{0}\end{bmatrix}}_{\mathcal{C}_\partial}\begin{pmatrix}\boldsymbol{e}_v \\ \boldsymbol{E}_\varepsilon\end{pmatrix}.$$

Outline

The Mindlin plate classical model

Model describing the bending deflection of **thick** plates of thickness h

$$
\begin{aligned}
\rho h \frac{\partial^2 w}{\partial t^2} &= \operatorname{div} \boldsymbol{q}, \qquad (x, y) \in \Omega \subset \mathbb{R}^2, \\
\frac{\rho h^3}{12} \frac{\partial^2 \boldsymbol{\theta}}{\partial t^2} &= \operatorname{Div} \boldsymbol{M} + \boldsymbol{q},
\end{aligned}
$$

Strains:

- $\boldsymbol{\kappa} = \operatorname{Grad} \boldsymbol{\theta}$ the curvature tensor;
- $\boldsymbol{\gamma} = \operatorname{grad} w - \boldsymbol{\theta}$ the shear strain.

Stresses:

- $\boldsymbol{M} = \boldsymbol{\mathcal{D}}_b \, \boldsymbol{\kappa}$ the momenta tensor;
- $\boldsymbol{\mathcal{D}}_b = \frac{E h^3}{12(1-\nu^2)} \left[(1-\nu)(\cdot) + \nu \operatorname{Tr}(\cdot) \boldsymbol{I}_{2\times 2}\right]$ the bending stiffness tensor;
- $\boldsymbol{q} = K_{\text{sh}} G h \, \boldsymbol{\gamma}$ the shear stress (G is the shear modulus and K_{sh} the shear correction factor);

Dirichlet conditions (clamped)		Neumann conditions (free)	
Vertical velocity	$w_t = \partial_t w$	Shear force	$q_n = \boldsymbol{q} \cdot \boldsymbol{n}$
Flexural rotation	$\omega_n = \partial_t \boldsymbol{\theta} \cdot \boldsymbol{n}$	Flexural momentum	$M_{nn} = \boldsymbol{n}^\top \boldsymbol{M} \boldsymbol{n}$
Torsional rotation	$\omega_s = \partial_t \boldsymbol{\theta} \cdot \boldsymbol{s}$	Torsional momentum	$M_{ns} = \boldsymbol{s}^\top \boldsymbol{M} \boldsymbol{n}$

Mixed condition: $w_t,\ \omega_s,\ M_{nn}$ given (simply supported)

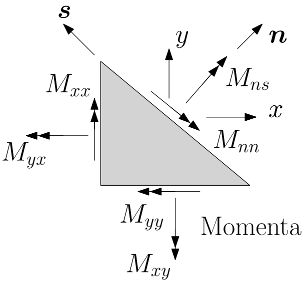

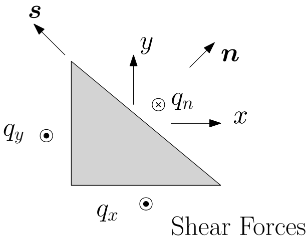

Energies and co-energies for the Mindlin plate

Total energy

$$H = \frac{1}{2} \int_{\Omega} \left\{ \rho h \left(\frac{\partial w}{\partial t} \right)^2 + \frac{\rho h^3}{12} \left\| \frac{\partial \boldsymbol{\theta}}{\partial t} \right\|^2 + \boldsymbol{M} : \boldsymbol{\kappa} + \boldsymbol{q} \cdot \boldsymbol{\gamma} \right\} \, \mathrm{d}\Omega,$$

Energy variables

$$\alpha_w = \rho h \frac{\partial w}{\partial t}, \quad \text{Linear momentum}, \qquad \boldsymbol{\alpha}_\theta = \frac{\rho h^3}{12} \frac{\partial \boldsymbol{\theta}}{\partial t}, \quad \text{Angular momentum},$$

$$\boldsymbol{A}_\kappa = \boldsymbol{\kappa}, \quad \text{Curvature tensor}, \qquad \boldsymbol{\alpha}_\gamma = \boldsymbol{\gamma}. \quad \text{Shear deformation}.$$

Co-energy variables

Interconnection operator and boundary variables

Dynamics

$$
\frac{\partial}{\partial t}\begin{pmatrix} \alpha_w \\ \boldsymbol{\alpha}_\theta \\ \boldsymbol{A}_\kappa \\ \boldsymbol{\alpha}_\gamma \end{pmatrix} = \underbrace{\begin{bmatrix} 0 & 0 & 0 & \mathrm{div} \\ \boldsymbol{0} & \boldsymbol{0} & \mathrm{Div} & \boldsymbol{I}_{2\times 2} \\ \boldsymbol{0} & \mathrm{Grad} & \boldsymbol{0} & \boldsymbol{0} \\ \mathrm{grad} & -\boldsymbol{I}_{2\times 2} & \boldsymbol{0} & \boldsymbol{0} \end{bmatrix}}_{\mathcal{J}} \begin{pmatrix} e_w \\ \boldsymbol{e}_\theta \\ \boldsymbol{E}_\kappa \\ \boldsymbol{e}_\gamma \end{pmatrix}.
$$

Boundary variables

$$
\begin{aligned}
\dot{H} &= \int_\Omega \left\{ \mathrm{div}(\boldsymbol{e}_\gamma) e_w + \mathrm{Div}(\boldsymbol{E}_\kappa) \cdot \boldsymbol{e}_\theta + \mathrm{Grad}(\boldsymbol{e}_\theta) : \boldsymbol{E}_\kappa + \mathrm{grad}(e_w) \cdot \boldsymbol{e}_\gamma \right\} \, \mathrm{d}\Omega, \\
&= \langle \gamma_0 e_w, \, \gamma_n \boldsymbol{e}_\gamma \rangle_{\partial\Omega} + \langle \gamma_n \boldsymbol{e}_\theta, \, \gamma_{nn} \boldsymbol{E}_\kappa \rangle_{\partial\Omega} + \langle \gamma_s \boldsymbol{e}_\theta, \, \gamma_{ns} \boldsymbol{E}_\kappa \rangle_{\partial\Omega},
\end{aligned}
$$

- $\gamma_{nn}\boldsymbol{E}_\kappa = \boldsymbol{n}^\top \boldsymbol{E}_\kappa \boldsymbol{n}|_{\partial\Omega}$ denotes the normal-normal trace of tensor-valued functions;
- $\gamma_{ns}\boldsymbol{E}_\kappa = \boldsymbol{s}^\top \boldsymbol{E}_\kappa \boldsymbol{n}|_{\partial\Omega}$ denotes the normal-tangential trace of tensor-valued functions.

PH Mindlin plate

$$\frac{\partial}{\partial t}\begin{pmatrix}\alpha_w \\ \boldsymbol{\alpha}_\theta \\ \boldsymbol{A}_\kappa \\ \boldsymbol{\alpha}_\gamma\end{pmatrix} = \underbrace{\begin{bmatrix} 0 & 0 & 0 & \mathrm{div} \\ \mathbf{0} & \mathbf{0} & \mathrm{Div} & \boldsymbol{I}_{2\times 2} \\ \mathbf{0} & \mathrm{Grad} & \mathbf{0} & \mathbf{0} \\ \mathrm{grad} & -\boldsymbol{I}_{2\times 2} & \mathbf{0} & \mathbf{0}\end{bmatrix}}_{\mathcal{J}} \begin{pmatrix} e_w \\ \boldsymbol{e}_\theta \\ \boldsymbol{E}_\kappa \\ \boldsymbol{e}_\gamma\end{pmatrix}, \qquad \begin{pmatrix} e_w \\ \boldsymbol{e}_\theta \\ \boldsymbol{E}_\kappa \\ \boldsymbol{e}_\gamma\end{pmatrix} = \underbrace{\begin{bmatrix} \frac{1}{\rho h} & 0 & 0 & 0 \\ \mathbf{0} & \frac{12}{\rho h^3} & \mathbf{0} & \mathbf{0} \\ \mathbf{0} & \mathbf{0} & \boldsymbol{\mathcal{D}}_b & \mathbf{0} \\ \mathbf{0} & \mathbf{0} & \mathbf{0} & K_{\mathsf{sh}} G h\end{bmatrix}}_{\mathcal{Q}} \begin{pmatrix}\alpha_w \\ \boldsymbol{\alpha}_\theta \\ \boldsymbol{A}_\kappa \\ \boldsymbol{\alpha}_\gamma\end{pmatrix},$$

$$\boldsymbol{u}_\partial = \underbrace{\begin{bmatrix} \gamma_0^{\Gamma_C} & 0 & 0 & 0 \\ 0 & \gamma_n^{\Gamma_C} & 0 & 0 \\ 0 & \gamma_s^{\Gamma_C} & 0 & 0 \\ \gamma_0^{\Gamma_S} & 0 & 0 & 0 \\ 0 & \gamma_s^{\Gamma_S} & 0 & 0 \\ 0 & 0 & \gamma_{nn}^{\Gamma_S} & 0 \\ 0 & 0 & \gamma_{nn}^{\Gamma_F} & 0 \\ 0 & 0 & \gamma_{ns}^{\Gamma_F} & 0 \\ 0 & 0 & 0 & \gamma_n^{\Gamma_F} \end{bmatrix}}_{\mathcal{B}_\partial} \begin{pmatrix} e_w \\ \boldsymbol{e}_\theta \\ \boldsymbol{E}_\kappa \\ \boldsymbol{e}_\gamma\end{pmatrix}, \qquad \boldsymbol{y}_\partial = \underbrace{\begin{bmatrix} 0 & 0 & 0 & \gamma_n^{\Gamma_C} \\ 0 & 0 & \gamma_{nn}^{\Gamma_C} & 0 \\ 0 & 0 & \gamma_{ns}^{\Gamma_C} & 0 \\ 0 & 0 & 0 & \gamma_n^{\Gamma_S} \\ 0 & 0 & \gamma_{ns}^{\Gamma_S} & 0 \\ 0 & \gamma_n^{\Gamma_S} & 0 & 0 \\ 0 & \gamma_n^{\Gamma_F} & 0 & 0 \\ 0 & \gamma_s^{\Gamma_F} & 0 & 0 \\ \gamma_0^{\Gamma_F} & 0 & 0 & 0 \end{bmatrix}}_{\mathcal{C}_\partial} \begin{pmatrix} e_w \\ \boldsymbol{e}_\theta \\ \boldsymbol{E}_\kappa \\ \boldsymbol{e}_\gamma\end{pmatrix}.$$

This model describes the bending deflection of **thin** plates

$$\rho h \frac{\partial^2 w}{\partial t^2} = -\operatorname{div} \operatorname{Div} \boldsymbol{M}, \qquad (x, y) \in \Omega \subset \mathbb{R}^2.$$

As for the Mindlin plate the stress tensor is defined as

$$\boldsymbol{M} = \boldsymbol{\mathcal{D}}_b \boldsymbol{\kappa}.$$

However, the curvature tensor is now given by the Hessian of the displacement field

$$\boldsymbol{\kappa} = \operatorname{Grad} \operatorname{grad} w = \operatorname{Hess} w.$$

Notice that $\operatorname{Grad} \circ \operatorname{grad} = \operatorname{Hess}$.

Dirichlet conditions (clamped)		Neumann conditions (free)	
Vertical velocity	w_t	Effective shear force	$\widetilde{q}_n = -\operatorname{Div} \boldsymbol{M} \cdot \boldsymbol{n} - \partial_{\boldsymbol{s}}(\boldsymbol{s}^\top \boldsymbol{M}\boldsymbol{n})$
Flexural rotation	$\partial_{\boldsymbol{n}} w_t$	Flexural momentum	$M_{nn} = \boldsymbol{n}^\top \boldsymbol{M}\boldsymbol{n}$

Mixed conditions: w_t, M_{nn} given (simply supported)

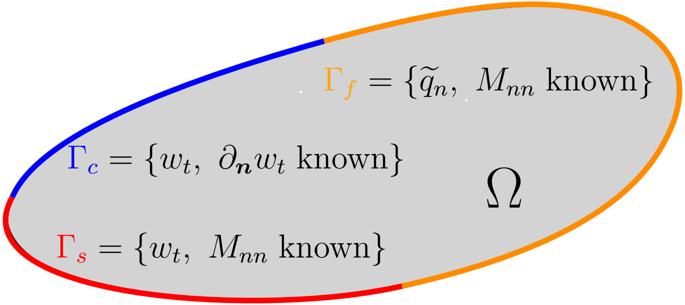

Energies and co-energies for the Kirchhoff plate

Total energy

$$H = \frac{1}{2} \int_{\Omega} \left\{ \rho h \left(\partial_t w\right)^2 + \boldsymbol{M} : \boldsymbol{\kappa} \right\} \, \mathrm{d}\Omega,$$

Energy variables

$$\alpha_w = \rho h \partial_t w, \quad \text{Linear momentum}, \qquad \boldsymbol{A}_\kappa = \boldsymbol{\kappa}, \quad \text{Curvature tensor.}$$

Co-energy variables

$$e_w := \frac{\delta H}{\delta \alpha_w} = \partial_t w, \quad \text{Linear velocity}, \qquad \boldsymbol{E}_\kappa := \frac{\delta H}{\delta \boldsymbol{A}_\kappa} = \boldsymbol{M}, \quad \text{Momenta tensor.}$$

Interconnection operator and boundary variables

Dynamics

$$\frac{\partial}{\partial t}\begin{pmatrix}\alpha_w \\ \boldsymbol{A}_\kappa\end{pmatrix} = \underbrace{\begin{bmatrix} 0 & -\operatorname{div}\circ\operatorname{Div} \\ \operatorname{Grad}\circ\operatorname{grad} & \boldsymbol{0}\end{bmatrix}}_{\mathcal{J}}\begin{pmatrix}e_w \\ \boldsymbol{E}_\kappa\end{pmatrix}.$$

Theorem

The formal adjoint of the $\operatorname{div}\operatorname{Div}$ operator is $\operatorname{Grad}\operatorname{grad}$, the Hessian operator.

Hence $\mathcal{J}$ is skew-symmetric.

Boundary variables

Assuming a regular boundary $\partial\Omega \in C^1$

$$\begin{aligned}\dot{H} &= \int_\Omega \left\{-\operatorname{div}\operatorname{Div}\boldsymbol{E}_\kappa\, e_w + \operatorname{Grad}\operatorname{grad} e_w : \boldsymbol{E}_\kappa\right\}\, \mathrm{d}\Omega, \\ &= \langle \gamma_0 e_w,\, \gamma_{nn,1}\boldsymbol{E}_\kappa\rangle_{\partial\Omega} + \langle \gamma_1 e_w,\, \gamma_{nn}\boldsymbol{E}_\kappa\rangle_{\partial\Omega}.\end{aligned}$$

- $\gamma_1 e_w = \partial_{\boldsymbol{n}} e_w|_{\partial\Omega}$ denote the normal derivative trace;
- $\gamma_{nn,1}$ denotes the map $\gamma_{nn,1}\boldsymbol{E}_\kappa = -\boldsymbol{n}\cdot\operatorname{Div}\boldsymbol{E}_\kappa - \partial_{\boldsymbol{s}}(\boldsymbol{s}^\top\boldsymbol{E}_\kappa\boldsymbol{n})|_{\partial\Omega}$.

PH Kirchhoff plate

$$\frac{\partial}{\partial t}\begin{pmatrix}\alpha_w \\ \boldsymbol{A}_\kappa\end{pmatrix} = \underbrace{\begin{bmatrix} 0 & -\operatorname{div}\circ\operatorname{Div} \\ \operatorname{Grad}\circ\operatorname{grad} & \boldsymbol{0}\end{bmatrix}}_{\mathcal{J}:\text{2nd order}}\begin{pmatrix}e_w \\ \boldsymbol{E}_\kappa\end{pmatrix}, \qquad \begin{pmatrix}e_w \\ \boldsymbol{E}_\kappa\end{pmatrix} = \underbrace{\begin{bmatrix}\frac{1}{\rho h} & 0 \\ \boldsymbol{0} & \boldsymbol{\mathcal{D}}_b\end{bmatrix}}_{\mathcal{Q}}\begin{pmatrix}\alpha_w \\ \boldsymbol{A}_\kappa\end{pmatrix},$$

$$\boldsymbol{u}_\partial = \underbrace{\begin{bmatrix} \gamma_0^{\Gamma_C} & 0 \\ \gamma_1^{\Gamma_C} & 0 \\ \gamma_0^{\Gamma_S} & 0 \\ 0 & \gamma_{nn}^{\Gamma_S} \\ 0 & \gamma_{nn,1}^{\Gamma_F} \\ 0 & \gamma_{nn}^{\Gamma_F}\end{bmatrix}}_{\mathcal{B}_\partial}\begin{pmatrix}e_w \\ \boldsymbol{E}_\kappa\end{pmatrix}, \qquad \boldsymbol{y}_\partial = \underbrace{\begin{bmatrix} 0 & \gamma_{nn,1}^{\Gamma_C} \\ 0 & \gamma_{nn}^{\Gamma_C} \\ 0 & \gamma_{nn,1}^{\Gamma_S} \\ \gamma_1^{\Gamma_S} & 0 \\ \gamma_0^{\Gamma_F} & 0 \\ \gamma_1^{\Gamma_F} & 0\end{bmatrix}}_{\mathcal{C}_\partial}\begin{pmatrix}e_w \\ \boldsymbol{E}_\kappa\end{pmatrix}.$$

Outline

Infinite-dimensional pH system

PDE with distributed inputs:

$$\frac{\partial \boldsymbol{\alpha}}{\partial t}(\boldsymbol{x}, t) = \mathcal{J}\delta_{\boldsymbol{\alpha}} H + \mathcal{B}\boldsymbol{u}_\Omega(\boldsymbol{x}, t),$$
$$\boldsymbol{y}_\Omega(\boldsymbol{x}, t) = \mathcal{B}^* \delta_{\boldsymbol{\alpha}} H.$$

Boundary conditions:

$$\boldsymbol{u}_\partial = \mathcal{B}_\partial \delta_{\boldsymbol{\alpha}} H, \qquad \boldsymbol{y}_\partial = \mathcal{C}_\partial \delta_{\boldsymbol{\alpha}} H.$$

Power balance (Stokes Theorem):

$$\dot{H} = \int_{\partial\Omega} \boldsymbol{u}_\partial \cdot \boldsymbol{y}_\partial \, \mathrm{d}S + \int_\Omega \boldsymbol{u}_\Omega \cdot \boldsymbol{y}_\Omega \, \mathrm{d}\Omega.$$

Structure-preserving discretization

Resulting ODE:

$$\dot{\boldsymbol{\alpha}}_d = \mathbf{J}\,\nabla H_d + \mathbf{B}_\Omega \mathbf{u}_\Omega + \mathbf{B}_\partial \mathbf{u}_\partial,$$
$$\mathbf{y}_\Omega = \mathbf{B}_\Omega^\top \nabla H_d,$$
$$\mathbf{y}_\partial = \mathbf{B}_\partial^\top \nabla H_d.$$

Discretized Hamiltonian:

$$H_d := H(\boldsymbol{\alpha} \equiv \boldsymbol{\alpha}_d).$$

Power balance:

$$\dot{H} = \mathbf{u}_\partial^\top \mathbf{y}_\partial + \mathbf{u}_\Omega^\top \mathbf{y}_\Omega.$$

Discretization of port-Hamiltonian system

Available methods

- Spectral methods (Moulla 2012):
  - ✓ Rapid spectral convergence;
  - × Only for 1D problem;
- Finite differences (Trenchant 2018):
  - ✓ Valid up to 2D geometries;
  - × Requires *ad hoc* implementation (staggered grids);
- Finite elements based
  - Golo 2004, Kotyczka 2018:
    - × they require tuning of some parameters to ensure the power flows preservation;
  - Cardoso-Ribeiro 2018:
    - ✓ Natural extension of the mixed finite element method to pH systems;
    - ✓ Implementable using well-established libraries (FEniCS, Firedrake);

Underlying hypotheses of the method

Assumption (Partitioned structure of the pH system)

The pH system has the partitioned form

$$\partial_t \begin{pmatrix} \boldsymbol{\alpha}_1 \\ \boldsymbol{\alpha}_2 \end{pmatrix} = \begin{bmatrix} 0 & -\mathcal{L}^* \\ \mathcal{L} & 0 \end{bmatrix} \begin{pmatrix} \boldsymbol{e}_1 \\ \boldsymbol{e}_2 \end{pmatrix}, \qquad \begin{pmatrix} \boldsymbol{e}_1 \\ \boldsymbol{e}_2 \end{pmatrix} := \begin{pmatrix} \delta_{\boldsymbol{\alpha}_1} H \\ \delta_{\boldsymbol{\alpha}_2} H \end{pmatrix},$$

$$\begin{aligned} \boldsymbol{\alpha}_1 &\in L^2(\Omega, \mathbb{A}), \\ \boldsymbol{\alpha}_2 &\in L^2(\Omega, \mathbb{B}), \\ \boldsymbol{e}_1 &\in H^{\mathcal{L}} := \left\{ \boldsymbol{u}_1 \in L^2(\Omega, \mathbb{A}) |\ \mathcal{L}\boldsymbol{u}_1 \in L^2(\Omega, \mathbb{B}) \right\}, \\ \boldsymbol{e}_2 &\in H^{-\mathcal{L}^*} := \left\{ \boldsymbol{u}_2 \in L^2(\Omega, \mathbb{B}) |\ -\mathcal{L}^*\boldsymbol{u}_2 \in L^2(\Omega, \mathbb{A}) \right\}. \end{aligned}$$

The sets $\mathbb{A}, \mathbb{B}$ are Cartesian product of either scalar, vectorial or tensorial quantities.

Wave-like equations (e.g. linear elastic models) possess this structure[12].

Assumption (Abstract integration by parts formula)

Assume that there exists two boundary operators $\mathcal{N}_{\partial,1}$, $\mathcal{N}_{\partial,2}$ such that a general integration by parts formula holds $\forall \boldsymbol{e}_1 \in H^{\mathcal{L}}$ and $\forall \boldsymbol{e}_2 \in H^{-\mathcal{L}^*}$

The partitioned finite element method

This discretization procedure boils down to three simple steps:

1. The system is written in weak form;
2. An integration by parts is applied to highlight the appropriate boundary control;
3. A Galerkin method is employed to obtain a finite-dimensional system. For the approximation basis the Finite Element Method FEM (large sparse matrices) is here employed but Spectral Methods SM (small full matrices) can be used as well.

Consider the causality

$$\boldsymbol{u}_\partial = \mathcal{N}_{\partial,1}\boldsymbol{e}_1, \qquad \boldsymbol{y}_\partial = \mathcal{N}_{\partial,2}\boldsymbol{e}_2.$$

By integrating by parts $\mathcal{L}$ the appropriate causality is obtained for the discretized system.

Finite dimensional system for $\boldsymbol{u}_\partial = \mathcal{N}_{\partial,1}\boldsymbol{e}_1$

$$\begin{bmatrix} \mathbf{M}_1 & \mathbf{0} \\ \mathbf{0} & \mathbf{M}_2 \end{bmatrix} \begin{pmatrix} \dot{\boldsymbol{\alpha}}_{d,1} \\ \dot{\boldsymbol{\alpha}}_{d,2} \end{pmatrix} = \begin{bmatrix} \mathbf{0} & \mathbf{D}_{-\mathcal{L}^*} \\ -\mathbf{D}_{-\mathcal{L}^*}^\top & \mathbf{0} \end{bmatrix} \begin{pmatrix} \mathbf{e}_1 \\ \mathbf{e}_2 \end{pmatrix} + \begin{bmatrix} \mathbf{0} \\ \mathbf{B}_2 \end{bmatrix} \mathbf{u}_\partial,$$

$$\begin{bmatrix} \mathbf{M}_1 & \mathbf{0} \\ \mathbf{0} & \mathbf{M}_2 \end{bmatrix} \begin{pmatrix} \mathbf{e}_1 \\ \mathbf{e}_2 \end{pmatrix} = \begin{pmatrix} \partial_{\boldsymbol{\alpha}_{d,1}} H_d(\boldsymbol{\alpha}_d) \\ \partial_{\boldsymbol{\alpha}_{d,2}} H_d(\boldsymbol{\alpha}_d) \end{pmatrix},$$

$$\mathbf{M}_\partial \mathbf{y}_\partial = \begin{bmatrix} \mathbf{0} & \mathbf{B}_2^\top \end{bmatrix} \begin{pmatrix} \mathbf{e}_1 \\ \mathbf{e}_2 \end{pmatrix}.$$

The discretized system

Consider the causality

$$\boldsymbol{u}_\partial = \mathcal{N}_{\partial,2}\boldsymbol{e}_2, \qquad \boldsymbol{y}_\partial = \mathcal{N}_{\partial,1}\boldsymbol{e}_1.$$

By integrating by parts $-\mathcal{L}^*$ the appropriate causality is obtained for the discretized system.

Finite dimensional system for $\boldsymbol{u}_\partial = \mathcal{N}_{\partial,2}\boldsymbol{e}_2$

$$\begin{bmatrix} \mathbf{M}_1 & \mathbf{0} \\ \mathbf{0} & \mathbf{M}_2 \end{bmatrix} \begin{pmatrix} \dot{\boldsymbol{\alpha}}_{d,1} \\ \dot{\boldsymbol{\alpha}}_{d,2} \end{pmatrix} = \begin{bmatrix} \mathbf{0} & -\mathbf{D}_{\mathcal{L}}^\top \\ \mathbf{D}_{\mathcal{L}} & \mathbf{0} \end{bmatrix} \begin{pmatrix} \mathbf{e}_1 \\ \mathbf{e}_2 \end{pmatrix} + \begin{bmatrix} \mathbf{B}_1 \\ \mathbf{0} \end{bmatrix} \mathbf{u}_\partial,$$

$$\begin{bmatrix} \mathbf{M}_1 & \mathbf{0} \\ \mathbf{0} & \mathbf{M}_2 \end{bmatrix} \begin{pmatrix} \mathbf{e}_1 \\ \mathbf{e}_2 \end{pmatrix} = \begin{bmatrix} \partial_{\boldsymbol{\alpha}_{d,1}} H_d(\boldsymbol{\alpha}_d) \\ \partial_{\boldsymbol{\alpha}_{d,2}} H_d(\boldsymbol{\alpha}_d) \end{bmatrix},$$

$$\mathbf{M}_\partial \mathbf{y}_\partial = \begin{bmatrix} \mathbf{B}_1^\top & \mathbf{0} \end{bmatrix} \begin{pmatrix} \mathbf{e}_1 \\ \mathbf{e}_2 \end{pmatrix}.$$

Discrete power balance

The power balance

$$\dot{H}_d = \partial^\top_{\boldsymbol{\alpha}_{d,1}} H_d(\boldsymbol{\alpha}_d)\dot{\boldsymbol{\alpha}}_{d,1} + \partial^\top_{\boldsymbol{\alpha}_{d,2}} H_d(\boldsymbol{\alpha}_d)\dot{\boldsymbol{\alpha}}_{d,2}$$

mimics the continuous one.

Causality $\boldsymbol{u}_\partial = \mathcal{N}_{\partial,1}\boldsymbol{e}_1$

$$\begin{aligned}\dot{H}_d &= \mathbf{e}_1^\top \mathbf{D}_{-\mathcal{L}^*}\mathbf{e}_2 - \mathbf{e}_2^\top \mathbf{D}_{-\mathcal{L}^*}^\top \mathbf{e}_1 + \mathbf{e}_2^\top \mathbf{B}_2 \mathbf{u}_\partial, \\ &= \mathbf{y}_\partial^\top \mathbf{M}_\partial \mathbf{u}_\partial\end{aligned}$$

Causality $\boldsymbol{u}_\partial = \mathcal{N}_{\partial,2}\boldsymbol{e}_2$

$$\begin{aligned}\dot{H}_d &= -\mathbf{e}_1^\top \mathbf{D}_{\mathcal{L}}^\top \mathbf{e}_2 + \mathbf{e}_2^\top \mathbf{D}_{\mathcal{L}} \mathbf{e}_1 + \mathbf{e}_1^\top \mathbf{B}_1 \mathbf{u}_\partial, \\ &= \mathbf{y}_\partial^\top \mathbf{M}_\partial \mathbf{u}_\partial.\end{aligned}$$

The final canonical system

Canonical representation

The constitutive relations have been discretized separately from the dynamics. A canonical pH system is obtained by matrix inversions.

$$\begin{pmatrix} \dot{\boldsymbol{\alpha}}_{d,1} \\ \dot{\boldsymbol{\alpha}}_{d,2} \end{pmatrix} = \underbrace{\begin{bmatrix} \mathbf{0} & \mathbf{M}_1^{-1}\mathbf{D}\mathbf{M}_2^{-1} \\ -\mathbf{M}_2^{-1}\mathbf{D}^\top\mathbf{M}_1^{-1} & \mathbf{0} \end{bmatrix}}_{\mathbf{J}} \begin{pmatrix} \partial_{\boldsymbol{\alpha}_{d,1}} H_d(\boldsymbol{\alpha}_d) \\ \partial_{\boldsymbol{\alpha}_{d,2}} H_d(\boldsymbol{\alpha}_d) \end{pmatrix} + \text{Boundary control.}$$

Numerical issues related to the canonical representation

Matrix inversions are unfeasible for large problems and generally speaking not recommended. However, for small-size problems ($N_{\text{dof}} \approx 10^4$) it is possible to obtain a canonical system ready for simulation.

α_h the fluid height, $\boldsymbol{\alpha}_v$ the linear momentum.

$$\frac{\partial}{\partial t}\begin{pmatrix}\alpha_h \\ \boldsymbol{\alpha}_v\end{pmatrix} = \begin{bmatrix} 0 & -\operatorname{div} \\ -\operatorname{grad} & \mathbf{0}\end{bmatrix}\begin{pmatrix} e_h \\ \boldsymbol{e}_v\end{pmatrix}, \qquad (x,y)\in\Omega = \{x^2+y^2 \leq R\},$$

$$\begin{pmatrix} e_h \\ \boldsymbol{e}_v\end{pmatrix} = \begin{pmatrix}\delta_{\alpha_h} H \\ \delta_{\boldsymbol{\alpha}_v} H\end{pmatrix} = \begin{pmatrix}\frac{1}{2\rho}\left\|\boldsymbol{\alpha}_v\right\|^2 + \rho g \alpha_h \\ \frac{1}{\rho}\alpha_h \boldsymbol{\alpha}_v\end{pmatrix},$$

The Hamiltonian is a non-quadratic and non-separable functional

$$H(\alpha_h, \boldsymbol{\alpha}_v) = \frac{1}{2}\int_\Omega \left\{\frac{1}{\rho}\alpha_h \left\|\boldsymbol{\alpha}_v\right\|^2 + \rho g \alpha_h^2\right\} \mathrm{d}\Omega.$$

Consider a uniform Neumann boundary control

$$u_\partial = -\boldsymbol{e}_v \cdot \boldsymbol{n}|_{\partial\Omega} = -\frac{1}{\rho}\alpha_h \boldsymbol{\alpha}_v \cdot \boldsymbol{n}|_{\partial\Omega}, \qquad \text{Volumetric inflow rate.}$$

The corresponding output reads

$$y_\partial = e_h|_{\partial\Omega} = (\rho g \alpha_h + \frac{1}{2\rho}\left\|\boldsymbol{\alpha}_v\right\|^2)|_{\partial\Omega}.$$

A simple proportional control stabilizes the system around the desired point h^{des}

$$u_\partial = -k(y_\partial - y_\partial^{\text{des}}), \qquad y_\partial^{\text{des}} = \rho g h^{\text{des}}, \quad k > 0.$$

This control law ensures that the Lyapunov functional

$$V = \frac{1}{2}\int_\Omega \left\{\frac{1}{2}\rho g(\alpha_h - \alpha_h^{\text{des}})^2 + \frac{1}{2\rho}\alpha_h \left\|\boldsymbol{\alpha}_v\right\|^2\right\} d\Omega \geq 0,$$

where $\alpha_h^{\text{des}} = h^{\text{des}}$, has negative semi definite time derivative

$$\dot{V} = -k\int_{\partial\Omega} \left(y_\partial - y_\partial^{\text{des}}\right)^2 \, \mathrm{d}\Gamma \leq 0.$$

Discretization strategy

- The div operator is integrated by parts to highlight the appropriate the Neumann boundary control.
- FEniCS is used to generate the matrices.

Parameters	
ρ	1000 [kg $\cdot$ m^3]
g	10 [m/s^2]
R	1 [m]
h^{des}	1 [m]

Simulation Settings	
Integrator	Runge-Kutta 45
N°_{dof}	3973
FE spaces	$(\alpha_h \approx \mathrm{CG}_1) \times (\boldsymbol{\alpha}_v \approx \mathrm{DG}_0) \times (u_\partial \approx \mathrm{DG}_0)$
t_{end}	3 [s]

Control parameter $$k = \begin{cases} 0, & \forall t < 0.5 \text{ [s]}, \\ 10^{-3}, & \forall t \geq 0.5 \text{ [s]}. \end{cases}$$

Results irrotational SWE

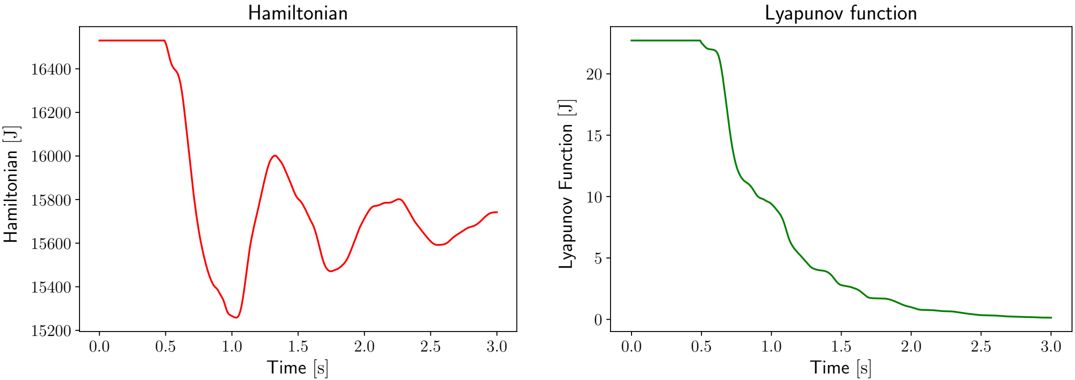

Outline

Assumption (Quadratic separable Hamiltonian)

The Hamiltonian is assumed to be a positive quadratic separable functional in $\boldsymbol{\alpha}_1, \boldsymbol{\alpha}_2$

$$H = \frac{1}{2} \langle \boldsymbol{\alpha}_1, \, \mathcal{Q}_1 \boldsymbol{\alpha}_1 \rangle_{L^2(\Omega, \mathbb{A})} + \frac{1}{2} \langle \boldsymbol{\alpha}_2, \, \mathcal{Q}_2 \boldsymbol{\alpha}_2 \rangle_{L^2(\Omega, \mathbb{B})},$$

where $\mathcal{Q}_1, \mathcal{Q}_2$ *are positive symmetric operators, bounded from below and above*

$$m_1 \boldsymbol{I}_{\mathbb{A}} \leq \mathcal{Q}_1 \leq M_1 \boldsymbol{I}_{\mathbb{A}}, \qquad m_2 \boldsymbol{I}_{\mathbb{B}} \leq \mathcal{Q}_2 \leq M_2 \boldsymbol{I}_{\mathbb{B}}, \qquad m_1 > 0, \; m_2 > 0, \; M_1 > 0, \; M_2 > 0.$$

PH linear system

$$\begin{bmatrix} \mathcal{M}_1 & 0 \\ 0 & \mathcal{M}_2 \end{bmatrix} \partial_t \begin{pmatrix} \boldsymbol{e}_1 \\ \boldsymbol{e}_2 \end{pmatrix} = \begin{bmatrix} 0 & -\mathcal{L}^* \\ \mathcal{L} & 0 \end{bmatrix} \begin{pmatrix} \boldsymbol{e}_1 \\ \boldsymbol{e}_2 \end{pmatrix}, \qquad \begin{aligned} \boldsymbol{e}_1 &\in H^{\mathcal{L}}, \\ \boldsymbol{e}_2 &\in H^{-\mathcal{L}^*}, \end{aligned}$$

where $\mathcal{M}_1 := \mathcal{Q}_1^{-1}$, $\mathcal{M}_2 := \mathcal{Q}_2^{-1}$. **Constitutive laws** have been included in the dynamics.

The linear discretized system

Finite dimensional system for $\boldsymbol{u}_\partial = \mathcal{N}_{\partial,1}\boldsymbol{e}_1, \; \boldsymbol{y}_\partial = \mathcal{N}_{\partial,2}\boldsymbol{e}_2$

$$
\begin{bmatrix}
\mathbf{M}_{\mathcal{M}_1} & \mathbf{0} \\
\mathbf{0} & \mathbf{M}_{\mathcal{M}_2}
\end{bmatrix}
\begin{pmatrix}
\dot{\mathbf{e}}_1 \\
\dot{\mathbf{e}}_2
\end{pmatrix}
=
\begin{bmatrix}
\mathbf{0} & \mathbf{D}_{-\mathcal{L}^*} \\
-\mathbf{D}_{-\mathcal{L}^*}^\top & \mathbf{0}
\end{bmatrix}
\begin{pmatrix}
\mathbf{e}_1 \\
\mathbf{e}_2
\end{pmatrix}
+
\begin{bmatrix}
\mathbf{0} \\
\mathbf{B}_2
\end{bmatrix}
\mathbf{u}_\partial,
$$

$$
\mathbf{M}_\partial \mathbf{y}_\partial =
\begin{bmatrix}
\mathbf{0} & \mathbf{B}_2^\top
\end{bmatrix}
\begin{pmatrix}
\mathbf{e}_1 \\
\mathbf{e}_2
\end{pmatrix}.
$$

Finite dimensional system for $\boldsymbol{u}_\partial = \mathcal{N}_{\partial,2}\boldsymbol{e}_2, \; \boldsymbol{y}_\partial = \mathcal{N}_{\partial,1}\boldsymbol{e}_1$

$$
\begin{bmatrix}
\mathbf{M}_{\mathcal{M}_1} & \mathbf{0} \\
\mathbf{0} & \mathbf{M}_{\mathcal{M}_2}
\end{bmatrix}
\begin{pmatrix}
\dot{\mathbf{e}}_1 \\
\dot{\mathbf{e}}_2
\end{pmatrix}
=
\begin{bmatrix}
\mathbf{0} & -\mathbf{D}_{\mathcal{L}}^\top \\
\mathbf{D}_{\mathcal{L}} & \mathbf{0}
\end{bmatrix}
\begin{pmatrix}
\mathbf{e}_1 \\
\mathbf{e}_2
\end{pmatrix}
+
\begin{bmatrix}
\mathbf{B}_1 \\
\mathbf{0}
\end{bmatrix}
\mathbf{u}_\partial,
$$

$$
\mathbf{M}_\partial \mathbf{y}_\partial =
\begin{bmatrix}
\mathbf{B}_1^\top & \mathbf{0}
\end{bmatrix}
\begin{pmatrix}
\mathbf{e}_1 \\
\mathbf{e}_2
\end{pmatrix}.
$$

The power balance

$$\dot{H}_d = \mathbf{e}_1^\top \mathbf{M}_{\mathcal{M}_1} \dot{\mathbf{e}}_1 + \mathbf{e}_2^\top \mathbf{M}_{\mathcal{M}_2} \dot{\mathbf{e}}_2$$

mimics the continuous one.

Causality $\boldsymbol{u}_\partial = \mathcal{N}_{\partial,1} \boldsymbol{e}_1$

$$\begin{aligned}\dot{H}_d &= \mathbf{e}_1^\top \mathbf{D}_{-\mathcal{L}^*} \mathbf{e}_2 - \mathbf{e}_2^\top \mathbf{D}_{-\mathcal{L}^*}^\top \mathbf{e}_1 + \mathbf{e}_2^\top \mathbf{B}_2 \mathbf{u}_\partial, \\ &= \mathbf{y}_\partial^\top \mathbf{M}_\partial \mathbf{u}_\partial\end{aligned}$$

Causality $\boldsymbol{u}_\partial = \mathcal{N}_{\partial,2} \boldsymbol{e}_2$

$$\begin{aligned}\dot{H}_d &= -\mathbf{e}_1^\top \mathbf{D}_{\mathcal{L}}^\top \mathbf{e}_2 + \mathbf{e}_2^\top \mathbf{D}_{\mathcal{L}} \mathbf{e}_1 + \mathbf{e}_1^\top \mathbf{B}_1 \mathbf{u}_\partial, \\ &= \mathbf{y}_\partial^\top \mathbf{M}_\partial \mathbf{u}_\partial.\end{aligned}$$

Outline

Consider now the following boundary-controlled linear pH system in co-energy form

$$\begin{bmatrix} \mathcal{M}_1 & 0 \\ 0 & \mathcal{M}_2 \end{bmatrix} \partial_t \begin{pmatrix} \boldsymbol{e}_1 \\ \boldsymbol{e}_2 \end{pmatrix} = \begin{bmatrix} 0 & -\mathcal{L}^* \\ \mathcal{L} & 0 \end{bmatrix} \begin{pmatrix} \boldsymbol{e}_1 \\ \boldsymbol{e}_2 \end{pmatrix},$$

$$\begin{pmatrix} \boldsymbol{u}_{\partial,1} \\ \boldsymbol{u}_{\partial,2} \end{pmatrix} = \begin{bmatrix} \mathcal{N}_{\partial,1}^{\Gamma_1} & 0 \\ 0 & \mathcal{N}_{\partial,2}^{\Gamma_2} \end{bmatrix} \begin{pmatrix} \boldsymbol{e}_1 \\ \boldsymbol{e}_2 \end{pmatrix},$$

$$\begin{pmatrix} \boldsymbol{y}_{\partial,1} \\ \boldsymbol{y}_{\partial,2} \end{pmatrix} = \begin{bmatrix} 0 & \mathcal{N}_{\partial,2}^{\Gamma_1} \\ \mathcal{N}_{\partial,1}^{\Gamma_2} & 0 \end{bmatrix} \begin{pmatrix} \boldsymbol{e}_1 \\ \boldsymbol{e}_2 \end{pmatrix}.$$

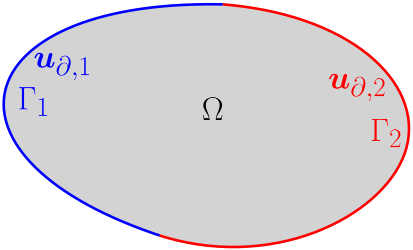

The operator $\mathcal{N}_{\partial,*}^{\Gamma_\circ}$ with $*, \circ \in \{1, 2\}$ represents the restriction of operator $\mathcal{N}_{\partial,*}$ over the subset $\Gamma_\circ \subset \partial\Omega$.

Mixed boundary conditions: two strategies

Lagrange multiplier

- ✓ Easier implementation (only one mesh);
- × Must fulfill the *inf-sup* condition;
- × Requires solving a DAE, or specific reduction methods.

Virtual domain decomposition

- ✓ Provides an ODE;
- × Requires the construction of multiple meshes;
- × Different formulation (and therefore finite elements) on each subdomain;

A Lagrange multiplier can be introduced to include the input that does not explicitly appear in the weak formulation, i.e. to enforce the essential boundary condition.

Integration by parts of $-\mathcal{L}^*$ ($\boldsymbol{\lambda}_{\partial,1} = \boldsymbol{y}_{\partial,1}$)

$$\mathrm{Diag}\begin{bmatrix} \mathbf{M}_{\mathcal{M}_1} \\ \mathbf{M}_{\mathcal{M}_2} \\ \mathbf{0} \end{bmatrix} \begin{pmatrix} \dot{\mathbf{e}}_1 \\ \dot{\mathbf{e}}_2 \\ \dot{\boldsymbol{\lambda}}_{\partial,1} \end{pmatrix} = \begin{bmatrix} \mathbf{0} & -\mathbf{D}_{\mathcal{L}}^\top & \mathbf{B}_{1,\Gamma_1} \\ \mathbf{D}_{\mathcal{L}} & \mathbf{0} & \mathbf{0} \\ -\mathbf{B}_{1,\Gamma_1}^\top & \mathbf{0} & \mathbf{0} \end{bmatrix} \begin{pmatrix} \mathbf{e}_1 \\ \mathbf{e}_2 \\ \boldsymbol{\lambda}_{\partial,1} \end{pmatrix} + \begin{bmatrix} \mathbf{0} & \mathbf{B}_{1,\Gamma_2} \\ \mathbf{0} & \mathbf{0} \\ \mathbf{M}_{\partial,1} & \mathbf{0} \end{bmatrix} \begin{bmatrix} \mathbf{u}_{\partial,1} \\ \mathbf{u}_{\partial,2} \end{bmatrix},$$

$$\begin{bmatrix} \mathbf{M}_{\partial,1} & \mathbf{0} \\ \mathbf{0} & \mathbf{M}_{\partial,2} \end{bmatrix} \begin{pmatrix} \mathbf{y}_{\partial,1} \\ \mathbf{y}_{\partial,2} \end{pmatrix} = \begin{bmatrix} \mathbf{0} & \mathbf{0} & \mathbf{M}_{\partial,1} \\ \mathbf{B}_{1,\Gamma_2}^\top & \mathbf{0} & \mathbf{0} \end{bmatrix} \begin{pmatrix} \mathbf{e}_1 \\ \mathbf{e}_2 \\ \boldsymbol{\lambda}_{\partial,1} \end{pmatrix}.$$

A Lagrange multiplier can be introduced to include the input that does not explicitly appear in the weak formulation, i.e. to enforce the essential boundary condition.

Integration by parts of $\mathcal{L}$ ($\boldsymbol{\lambda}_{\partial,2} = \boldsymbol{y}_{\partial,2}$)

$$
\mathrm{Diag}\begin{bmatrix}\mathbf{M}_{\mathcal{M}_1}\\ \mathbf{M}_{\mathcal{M}_2}\\ \mathbf{0}\end{bmatrix}\begin{pmatrix}\dot{\mathbf{e}}_1\\ \dot{\mathbf{e}}_2\\ \dot{\boldsymbol{\lambda}}_{\partial,2}\end{pmatrix} = \begin{bmatrix}\mathbf{0} & \mathbf{D}_{-\mathcal{L}^*} & \mathbf{0}\\ -\mathbf{D}_{-\mathcal{L}^*}^\top & \mathbf{0} & \mathbf{B}_{2,\Gamma_2}\\ \mathbf{0} & -\mathbf{B}_{2,\Gamma_2}^\top & \mathbf{0}\end{bmatrix}\begin{pmatrix}\mathbf{e}_1\\ \mathbf{e}_2\\ \boldsymbol{\lambda}_{\partial,2}\end{pmatrix} + \begin{bmatrix}\mathbf{0} & \mathbf{0}\\ \mathbf{B}_{2,\Gamma_1} & \mathbf{0}\\ \mathbf{0} & \mathbf{M}_{\partial,2}\end{bmatrix}\begin{bmatrix}\mathbf{u}_{\partial,1}\\ \mathbf{u}_{\partial,2}\end{bmatrix},
$$

$$
\begin{bmatrix}\mathbf{M}_{\partial,1} & \mathbf{0}\\ \mathbf{0} & \mathbf{M}_{\partial,2}\end{bmatrix}\begin{pmatrix}\mathbf{y}_{\partial,1}\\ \mathbf{y}_{\partial,2}\end{pmatrix} = \begin{bmatrix}\mathbf{0} & \mathbf{B}_{2,\Gamma_1}^\top & \mathbf{0}\\ \mathbf{0} & \mathbf{0} & \mathbf{M}_{\partial,2}\end{bmatrix}\begin{pmatrix}\mathbf{e}_1\\ \mathbf{e}_2\\ \boldsymbol{\lambda}_{\partial,2}\end{pmatrix}.
$$

A pH differential-algebraic system is obtained in this case (pHDAE).

The energy balance

$$\dot{H}_d = \mathbf{e}_1^\top \mathbf{M}_{\mathcal{M}_1} \dot{\mathbf{e}}_1 + \mathbf{e}_2^\top \mathbf{M}_{\mathcal{M}_2} \dot{\mathbf{e}}_2$$

mimics the continuous counterpart.

Integration by parts of $-\mathcal{L}^*$ ($\boldsymbol{\lambda}_{\partial,1} = \boldsymbol{u}_{\partial,1}$)

$$\begin{aligned}\dot{H}_d &= -\mathbf{e}_1^\top \mathbf{D}_{\mathcal{L}}^\top \mathbf{e}_2 + \mathbf{e}_2^\top \mathbf{D}_{\mathcal{L}} \mathbf{e}_1 + \mathbf{e}_1^\top (\mathbf{B}_{1,\Gamma_1} \boldsymbol{\lambda}_{\partial,1} + \mathbf{B}_{1,\Gamma_2} \mathbf{u}_{\partial,2}),\\ &= \mathbf{y}_{\partial,1}^\top \mathbf{M}_{\partial,1} \mathbf{u}_{\partial,1} + \mathbf{y}_{\partial,2}^\top \mathbf{M}_{\partial,2} \mathbf{u}_{\partial,2}.\end{aligned}$$

Integration by parts of $\mathcal{L}$ ($\boldsymbol{\lambda}_{\partial,2} = \boldsymbol{u}_{\partial,2}$)

$$\begin{aligned}\dot{H}_d &= \mathbf{e}_1^\top \mathbf{D}_{-\mathcal{L}^*}^\top \mathbf{e}_2 - \mathbf{e}_2^\top \mathbf{D}_{-\mathcal{L}^*} \mathbf{e}_1 + \mathbf{e}_2^\top (\mathbf{B}_{2,\Gamma_2} \boldsymbol{\lambda}_{\partial,2} + \mathbf{B}_{2,\Gamma_1} \mathbf{u}_{\partial,1}),\\ &= \mathbf{y}_{\partial,1}^\top \mathbf{M}_{\partial,1} \mathbf{u}_{\partial,1} + \mathbf{y}_{\partial,2}^\top \mathbf{M}_{\partial,2} \mathbf{u}_{\partial,2}.\end{aligned}$$

Example: cantilever Kirchhoff plate

$$\begin{bmatrix} \rho h & 0 \\ \mathbf{0} & \boldsymbol{\mathcal{D}}_b^{-1} \end{bmatrix} \frac{\partial}{\partial t} \begin{pmatrix} e_w \\ \boldsymbol{E}_\kappa \end{pmatrix} = \begin{bmatrix} 0 & -\operatorname{div}\operatorname{Div} \\ \operatorname{Grad}\operatorname{grad} & \mathbf{0} \end{bmatrix} \begin{pmatrix} e_w \\ \boldsymbol{E}_\kappa \end{pmatrix} \qquad (x, y) \in \Omega = [0, 1] \times [0, 1],$$

subject to Dirichlet homogeneous conditions and Neumann boundary control

$$\begin{aligned} \partial_t e_w|_{\Gamma_D} &= 0, \\ \partial_x e_w|_{\Gamma_D} &= 0, \end{aligned} \qquad \Gamma_D = \{x = 0\}, \qquad \begin{aligned} u_{\partial,q} &= \widetilde{q}_n|_{\Gamma_N}, \\ u_{\partial,m} &= M_{nn}|_{\Gamma_N}. \end{aligned} \qquad \Gamma_N = \{y = 0 \cup x = 1 \cup y = 1\}.$$

The corresponding boundary outputs read

$$\begin{aligned} y_{\partial,q} &= e_w|_{\Gamma_N}, \\ y_{\partial,m} &= \partial_{\boldsymbol{n}} e_w|_{\Gamma_N}. \end{aligned}$$

The following control law stabilizes the system

$$\begin{aligned} u_{\partial,q} &= -k y_{\partial,q}, \\ u_{\partial,m} &= -k y_{\partial,m}, \end{aligned} \qquad k > 0.$$

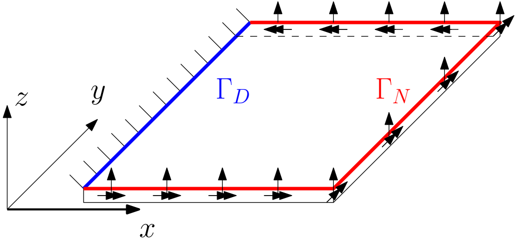

Discretization strategy

- The $\mathrm{div}\,\mathrm{Div}$ operator is integrated by parts twice to enforce weekly the Neumann bc.
- The FIREDRAKE library is used to generate the matrices.
- The Dirichlet condition is imposed weakly through a Lagrange multiplier (strong imposition of boundary conditions for H^2 conforming elements is not trivial[13]).

Plate Parameters	
E	70 [GPa]
ρ	$2700\ [\mathrm{kg} \cdot \mathrm{m}^3]$
ν	0.35
h/L	0.05
$L_x = L_y$	1 [m]

Simulation Settings	
Integrator	Störmer-Verlet
Δt	$1\ [\mu\mathrm{s}]$
$\mathrm{N}^\circ_{\mathrm{dof}}$	2574
FE spaces	$(e_w \approx \text{Argyris}) \times (\boldsymbol{E}_\kappa \approx \mathrm{DG}_3) \times (\boldsymbol{\lambda} \approx \mathrm{CG}_2)$
t_{end}	5 [s]

Control parameter $$k = \begin{cases} 0, & \forall t < 1\,[\mathrm{s}], \\ 10, & \forall t \geq 1\,[\mathrm{s}]. \end{cases}$$

[13] R.C. Kirby and L. Mitchell. "Code Generation for Generally Mapped Finite Elements". In: *ACM Trans. Math. Softw.* 45.4 (Dec. 2019).

Results cantilever Kirchoff plate

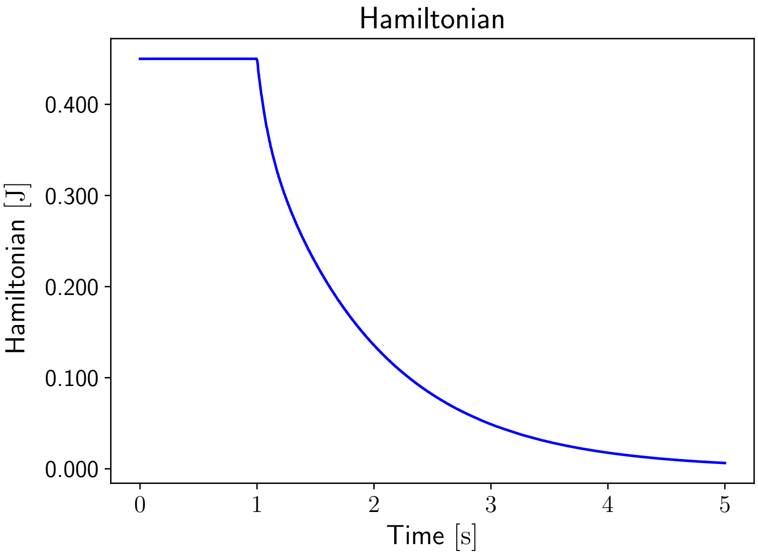

Outline

$$\begin{bmatrix} \rho b & 0 & 0 & 0 \\ \mathbf{0} & I_\theta & \mathbf{0} & \mathbf{0} \\ \mathbf{0} & \mathbf{0} & \boldsymbol{\mathcal{C}}_b & \mathbf{0} \\ \mathbf{0} & \mathbf{0} & \mathbf{0} & C_s \end{bmatrix} \frac{\partial}{\partial t} \begin{pmatrix} e_w \\ \boldsymbol{e}_\theta \\ \boldsymbol{E}_\kappa \\ \boldsymbol{e}_\gamma \end{pmatrix} = \begin{bmatrix} 0 & 0 & 0 & \mathrm{div} \\ \mathbf{0} & \mathbf{0} & \mathrm{Div} & \boldsymbol{I}_{2\times 2} \\ \mathbf{0} & \mathrm{Grad} & \mathbf{0} & \mathbf{0} \\ \mathrm{grad} & -\boldsymbol{I}_{2\times 2} & \mathbf{0} & \mathbf{0} \end{bmatrix} \begin{pmatrix} e_w \\ \boldsymbol{e}_\theta \\ \boldsymbol{E}_\kappa \\ \boldsymbol{e}_\gamma \end{pmatrix} + \begin{pmatrix} f \\ \boldsymbol{\tau} \\ \mathbf{0} \\ \mathbf{0} \end{pmatrix}, \qquad \begin{aligned} e_w|_{\partial\Omega} &= 0, \\ \boldsymbol{e}_\theta|_{\partial\Omega} &= \mathbf{0}. \end{aligned}$$

where b is the thickness, I_θ is the rotary inertia, $\boldsymbol{C}_b$, C_s are the bending and shear compliance respectively, f, $\boldsymbol{\tau}$ are distributed forces and torques.

For this example, the $\mathcal{L}$, $-\mathcal{L}^*$, $\mathcal{N}_{\partial,1}$, $\mathcal{N}_{\partial,2}$ operators are given by

$$\mathcal{L} = \begin{bmatrix} \mathbf{0} & \mathrm{Grad} \\ \mathrm{grad} & -\boldsymbol{I}_{2\times 2} \end{bmatrix}, \quad -\mathcal{L}^* = \begin{bmatrix} \mathbf{0} & \mathrm{div} \\ \mathrm{Div} & \boldsymbol{I}_{2\times 2} \end{bmatrix}, \qquad \mathcal{N}_{\partial,1} = \begin{bmatrix} \gamma_0 & 0 \\ 0 & \boldsymbol{\gamma}_0 \end{bmatrix}, \quad \mathcal{N}_{\partial,2} = \begin{bmatrix} 0 & \gamma_n \\ \boldsymbol{\gamma}_n & 0 \end{bmatrix}.$$

Mixed discretization

After integrating by parts $\mathcal{L}$, the weak form looks for solutions in the space

$$\{e_w, \boldsymbol{e_\theta}, \boldsymbol{E}_\kappa, \boldsymbol{e}_\gamma\} \in L^2(\Omega) \times L^2(\Omega, \mathbb{R}^2) \times H^{\mathrm{Div}}(\Omega, \mathbb{R}^{2\times 2}_{\mathsf{sym}}) \times H^{\mathrm{div}}(\Omega, \mathbb{R}^2).$$

The clamped condition is a natural one in this setting.

BJT elements

These elements were proposed in Bécache 2001 for elastodynamics problems[14].

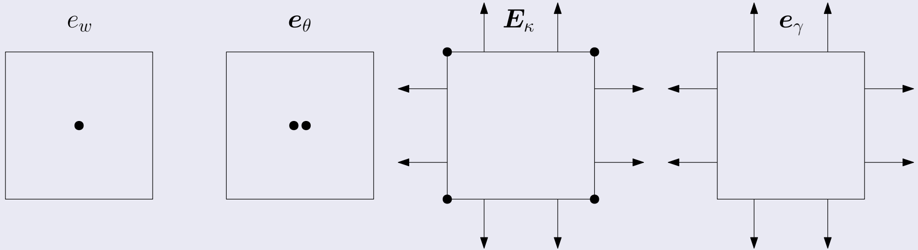

[14] E. Bécache, P. Joly, and C. Tsogka. "A New Family of Mixed Finite Elements for the Linear Elastodynamic Problem". In: *SIAM Journal on Numerical Analysis* 39 (June 2001), pp. 2109–2132.

Dual mixed formulation

If instead $-\mathcal{L}^*$ the weak form looks for solutions in the space

$$\{e_w, \boldsymbol{e_\theta}, \boldsymbol{E}_\kappa, \boldsymbol{e}_\gamma\} \in H^1(\Omega) \times H^{\mathrm{Grad}}(\Omega, \mathbb{R}^2) \times L^2(\Omega, \mathbb{R}^{2\times 2}_{\mathsf{sym}}) \times L^2(\Omega, \mathbb{R}^2).$$

The clamped condition is an essential one in this setting.

CG elements

Conforming elements for a similar problem are detailed in Cohen 2007[15].

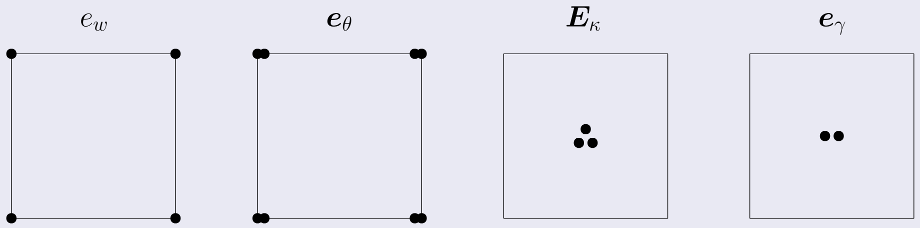

[15] G. Cohen and P. Grob. "Mixed Higher Order Spectral Finite Elements for Reissner–Mindlin Equations". In: *SIAM Journal on Scientific Computing* 29.3 (2007), pp. 986–1005.

Conjectured convergence estimates

Conjecture (Convergence rate for the BJT elements)

Combining previous results[16] *and assuming a smooth solution, the following error estimates hold (k polynomial degree for FE)*

$$||e_w - e_w^h||_{L^\infty(L^2(\Omega))} \lesssim h^k, \qquad ||\boldsymbol{E}_\kappa - \boldsymbol{E}_\kappa^h||_{L^\infty(L^2(\Omega,\mathbb{R}^{2\times 2}_{\mathrm{sym}}))} \lesssim h^k,$$
$$||\boldsymbol{e}_\theta - \boldsymbol{e}_\theta^h||_{L^\infty(L^2(\Omega,\mathbb{R}^2))} \lesssim h^k, \qquad ||\boldsymbol{e}_\gamma - \boldsymbol{e}_\gamma^h||_{L^\infty(L^2(\Omega,\mathbb{R}^2))} \lesssim h^k.$$

Conjecture (Convergence of the CG elements)

Assuming a smooth solution, the following error estimates hold (k polynomial degree for FE)

$$||e_w - e_w^h||_{L^\infty(H^1(\Omega))} \lesssim h^k, \qquad ||\boldsymbol{E}_\kappa - \boldsymbol{E}_\kappa^h||_{L^\infty(L^2(\Omega,\mathbb{R}^{2\times 2}_{\mathrm{sym}}))} \lesssim h^k,$$
$$||\boldsymbol{e}_\theta - \boldsymbol{e}_\theta^h||_{L^\infty(H^{\mathrm{Grad}}(\Omega,\mathbb{R}^2))} \lesssim h^k, \qquad ||\boldsymbol{e}_\gamma - \boldsymbol{e}_\gamma^h||_{L^\infty(L^2(\Omega,\mathbb{R}^2))} \lesssim h^k.$$

[16] E. Bécache, P. Joly, and C. Tsogka. “An Analysis of New Mixed Finite Elements for the Approximation of Wave Propagation Problems”. In: *SIAM Journal on Numerical Analysis* 37.4 (2000), pp. 1053–1084, E. Bécache, P. Joly, and C. Tsogka. “A New Family of Mixed Finite Elements for the Linear Elastodynamic Problem”. In: *SIAM Journal on Numerical Analysis* 39 (June 2001), pp. 2109–2132.

Simulation Settings

- The FIREDRAKE library is used to generate the matrices.
- Time integration: a Crank-Nicholson scheme has been used with time step $\Delta t = h/10$ where h is the mesh size.
- Linear solver: Conjugate gradient with LU preconditioner (ILU).
- To compute the $L^\infty(X)$ space-time dependent norm the discrete norm $L^\infty_{\Delta t}(X)$ is used

$$||\cdot||_{L^\infty(X)} \approx ||\cdot||_{L^\infty_{\Delta t}(X)} = \max_{t \in t_i} ||\cdot||_X, \qquad t_i \text{ are the discrete simulation instants.}$$

Plate parameters				
E	ρ	ν	K_{sh}	b
74 [GPa]	2700 [kg/m^3]	0.3	$5/6$	0.1 [m]

Table: Physical parameters for the Numerical test (Aluminum).

Results

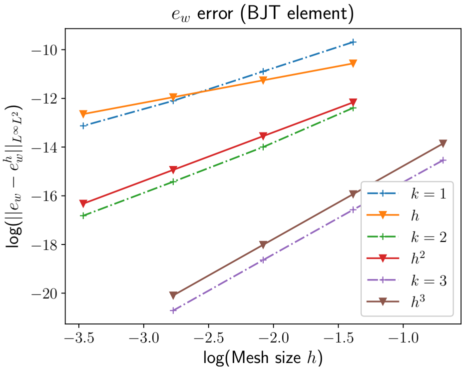

Figure: BTJ e_w error $(L^\infty(L^2(\Omega)))$.

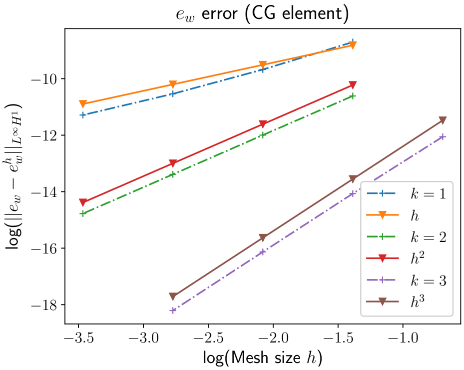

Figure: CG e_w error $(L^\infty(H^1(\Omega)))$.

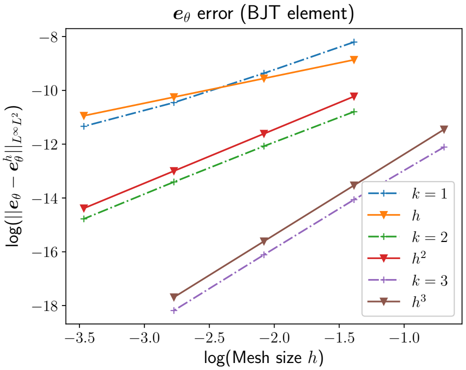

Figure: BTJ e_θ error $(L^\infty(L^2(\Omega, \mathbb{R}^2)))$.

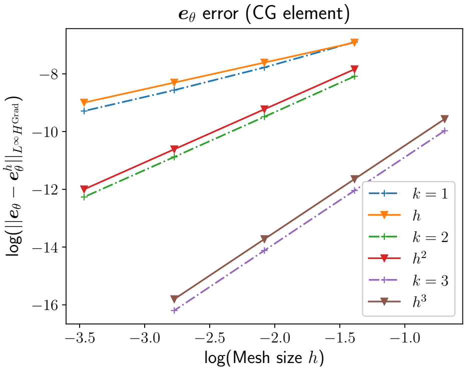

Figure: CG e_θ error $(L^\infty(H^{\mathrm{Grad}}(\Omega, \mathbb{R}^2)))$.

Outline

Previous work

Using Lie Algebra and differential forms a pH model of a flexible link has already been proposed[17]. This model can be embedded in a complex multibody system[18].

Advantages:

- Modular construction of flexible systems;
- Large deformations naturally considered.

Drawbacks:

- Quite cumbersome implementation;
- Limited to one-dimensional beam;
- Numerical analysis not feasible;
- Model reduction techniques not easily applicable.

[17] A. Macchelli, C. Melchiorri, and S. Stramigioli. "Port-Based Modeling of a Flexible Link". In: *IEEE Transactions on Robotics* 23 (2007), pp. 650 –660.

[18] A. Macchelli, C. Melchiorri, and S. Stramigioli. "Port-Based Modeling and Simulation of Mechanical Systems With Rigid and Flexible Links". In: *IEEE Transactions on Robotics* 25.5 (2009), pp. 1016–1029.

Floating frame of reference approach

The elastic motion is described in a reference frame that follows the large rigid motion.

Advantages

- Most used paradigm in multibody dynamics;
- For control other approaches are too complex;
- Linear model reduction techniques are applicable.

Drawbacks:

- Not suitable for large deformations.

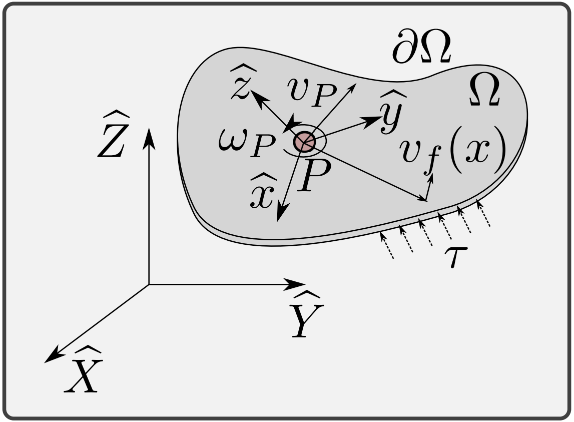

Floating body kinematics

The velocity of a generic point is expressed by considering a small flexible displacement superimposed to the rigid motion

$$\boldsymbol{v} = \boldsymbol{v}_P + [\boldsymbol{\omega}_P]_\times (\boldsymbol{x} + \boldsymbol{u}_f) + \boldsymbol{v}_f.$$

where the cross map $[\boldsymbol{a}]_\times$ denotes the skew-symmetric matrix associated to vector $\boldsymbol{a}$. This equation is expressed in the body reference frame $\widehat{\boldsymbol{x}}, \widehat{\boldsymbol{y}}, \widehat{\boldsymbol{z}}$.

Kinematic variables:

- $\boldsymbol{x}$ is the position vector of the current point;
- $\boldsymbol{v}_P$, $\boldsymbol{\omega}_P$ are the linear and angular velocities of point P;
- $\boldsymbol{v}_f := \dot{\boldsymbol{u}}_f$ the deformation velocity.

Inertia terms:

- $m := \int_\Omega \rho \, \mathrm{d}\Omega$ the total mass;
- $\boldsymbol{s}_u := \int_\Omega \rho(\boldsymbol{x} + \boldsymbol{u}_f) \, \mathrm{d}\Omega$ the static moment;
- $\boldsymbol{J}_u := \int_\Omega \rho \, [\boldsymbol{x} + \boldsymbol{u}_f]_\times^\top [\boldsymbol{x} + \boldsymbol{u}_f]_\times \, \mathrm{d}\Omega$ the inertia matrix.

Canonical momenta

Consider the total energy (Hamiltonian), given by the sum of kinetic and deformation energy:

$$H = H_{\text{kin}} + H_{\text{def}} = \frac{1}{2}\int_{\Omega} \left\{\rho||\boldsymbol{v}_P + [\boldsymbol{\omega}_P]_\times (\boldsymbol{x} + \boldsymbol{u}_f) + \boldsymbol{v}_f||^2 + \boldsymbol{\Sigma} : \boldsymbol{\varepsilon}\right\} \, \mathrm{d}\Omega.$$

Canonical momenta

$$\begin{aligned}
\boldsymbol{p}_t &:= \frac{\partial H}{\partial \boldsymbol{v}_P} = m\boldsymbol{v}_P + [\boldsymbol{s}_u]_\times^\top \boldsymbol{\omega}_P + \int_\Omega \rho \boldsymbol{v}_f \, \mathrm{d}\Omega, \\
\boldsymbol{p}_r &:= \frac{\partial H}{\partial \boldsymbol{\omega}_P} = [\boldsymbol{s}_u]_\times \boldsymbol{v}_P + \boldsymbol{J}_u \boldsymbol{\omega}_P + \int_\Omega \rho \, [\boldsymbol{x} + \boldsymbol{u}_f]_\times \boldsymbol{v}_f \, \mathrm{d}\Omega, \\
\boldsymbol{p}_f &:= \frac{\delta H}{\delta \boldsymbol{v}_f} = \rho \boldsymbol{v}_P + \rho \, [\boldsymbol{x} + \boldsymbol{u}_f]_\times^\top \boldsymbol{\omega}_P + \rho \boldsymbol{v}_f, \\
\boldsymbol{\varepsilon} &:= \frac{\delta H}{\delta \boldsymbol{\Sigma}} = \boldsymbol{\mathcal{D}}^{-1} \boldsymbol{\Sigma},
\end{aligned}$$

Canonical momenta

Consider the total energy (Hamiltonian), given by the sum of kinetic and deformation energy:

$$H = H_{\text{kin}} + H_{\text{def}} = \frac{1}{2}\int_\Omega \left\{\rho||\boldsymbol{v}_P + [\boldsymbol{\omega}_P]_\times (\boldsymbol{x} + \boldsymbol{u}_f) + \boldsymbol{v}_f||^2 + \boldsymbol{\Sigma} : \boldsymbol{\varepsilon}\right\} \, \mathrm{d}\Omega.$$

Canonical momenta

$$\begin{bmatrix} \boldsymbol{p}_t \\ \boldsymbol{p}_r \\ \boldsymbol{p}_f \\ \boldsymbol{\varepsilon} \end{bmatrix} = \underbrace{\begin{bmatrix} m\boldsymbol{I}_{3\times3} & [\boldsymbol{s}_u]_\times^\top & \mathcal{I}_\rho^\Omega & 0 \\ [\boldsymbol{s}_u]_\times & \boldsymbol{J}_u & \boldsymbol{\mathcal{I}}_{\rho x}^\Omega & 0 \\ (\mathcal{I}_\rho^\Omega)^* & (\boldsymbol{\mathcal{I}}_{\rho x}^\Omega)^* & \rho & 0 \\ 0 & 0 & 0 & \boldsymbol{\mathcal{D}}^{-1} \end{bmatrix}}_{\mathcal{M}:\ \text{Mass operator}} \begin{bmatrix} \boldsymbol{v}_P \\ \boldsymbol{\omega}_P \\ \boldsymbol{v}_f \\ \boldsymbol{\Sigma} \end{bmatrix}, \qquad \begin{aligned} \mathcal{I}_\rho^\Omega &:= \int_\Omega \rho(\cdot) \, \mathrm{d}\Omega, \\ \boldsymbol{\mathcal{I}}_{\rho x}^\Omega &:= \int_\Omega \rho \, [\boldsymbol{x} + \boldsymbol{u}_f]_\times (\cdot). \end{aligned}$$

The mass operator $\mathcal{M}$ is a self-adjoint, positive operator. It holds

$$H_{\text{kin}} + H_{\text{def}} = \frac{1}{2}\langle \boldsymbol{e}_{\text{kd}}, \ \mathcal{M}\boldsymbol{e}_{\text{kd}}\rangle, \qquad \boldsymbol{e}_{\text{kd}} = [\boldsymbol{v}_P; \, \boldsymbol{\omega}_P; \, \boldsymbol{v}_f; \boldsymbol{\Sigma}]$$

Canonical momenta

Consider the total energy (Hamiltonian), given by the sum of kinetic and deformation energy:

$$H = H_{\mathsf{kin}} + H_{\mathsf{def}} = \frac{1}{2}\int_\Omega \left\{\rho ||\boldsymbol{v}_P + [\boldsymbol{\omega}_P]_\times (\boldsymbol{x} + \boldsymbol{u}_f) + \boldsymbol{v}_f||^2 + \boldsymbol{\Sigma} : \boldsymbol{\varepsilon}\right\} \, \mathrm{d}\Omega.$$

Modified canonical momenta

$$\widehat{\boldsymbol{p}}_t := m\boldsymbol{v}_P + [\boldsymbol{s}_u]_\times^\top \boldsymbol{\omega}_P + 2\int_\Omega \rho \boldsymbol{v}_f \, \mathrm{d}\Omega, \qquad \widehat{\boldsymbol{p}}_f := \rho \boldsymbol{v}_P + \rho\, [\boldsymbol{x} + \boldsymbol{u}_f]_\times^\top \boldsymbol{\omega}_P + 2\rho \boldsymbol{v}_f,$$

$$\widehat{\boldsymbol{p}}_r := [\boldsymbol{s}_u]_\times \boldsymbol{v}_P + \boldsymbol{J}_u \boldsymbol{\omega}_P + 2\int_\Omega \rho\, [\boldsymbol{x} + \boldsymbol{u}_f]_\times \boldsymbol{v}_f \, \mathrm{d}\Omega, \qquad \boldsymbol{\mathcal{I}}_{p_f}^\Omega := \int_\Omega \left\{[\boldsymbol{p}_f]_\times + [\widehat{\boldsymbol{p}}_f]_\times\right\} (\cdot) \, \mathrm{d}\Omega,$$

Notice that the kinetic energy also depends on the flexible displacement

$$\frac{\delta H_{\mathsf{kin}}}{\delta \boldsymbol{u}_f} = [\boldsymbol{p}_f]_\times \boldsymbol{\omega}_P.$$

Generalized coordinates are required for a complete formulation:

- ${}^{i}\boldsymbol{r}_P$ the position of point P in the inertial frame of reference;
- $\boldsymbol{R}$ the direction cosine matrix (other attitude parametrizations are possible);
- $\boldsymbol{u}_f$ the flexible displacement;

The direction cosine matrix is converted into a vector by concatenating its rows

$$\boldsymbol{R}_{\mathsf{v}} = \mathrm{vec}(\boldsymbol{R}^\top) = [\boldsymbol{R}_1 \ \boldsymbol{R}_2 \ \boldsymbol{R}_3]^\top,$$

where $\boldsymbol{R}_1, \boldsymbol{R}_2, \boldsymbol{R}_3$ are the rows of matrix $\boldsymbol{R}$. Furthermore the corresponding cross map will be given by

$$[\boldsymbol{R}_{\mathsf{v}}]_\times = \begin{bmatrix} [\boldsymbol{R}_1]_\times \\ [\boldsymbol{R}_2]_\times \\ [\boldsymbol{R}_3]_\times \end{bmatrix}, \qquad [\boldsymbol{R}_{\mathsf{v}}]_\times : \mathbb{R}^9 \rightarrow \mathbb{R}^{9\times 3}.$$

The overall port-Hamiltonian formulation (without including the boundary traction $\boldsymbol{\tau}$)

$$
\underbrace{\left[\begin{array}{c:c} \boldsymbol{I} & 0 \\ \hdashline 0 & \mathcal{M} \end{array}\right]}_{\mathcal{E}} \frac{\partial}{\partial t} \underbrace{\begin{bmatrix} {}^{i}\boldsymbol{r}_P \\ \boldsymbol{R}_{\mathsf{v}} \\ \boldsymbol{u}_f \\ \hdashline \boldsymbol{v}_P \\ \boldsymbol{\omega}_P \\ \boldsymbol{v}_f \\ \boldsymbol{\Sigma} \end{bmatrix}}_{\boldsymbol{e}} = \underbrace{\left[\begin{array}{ccc:cccc} 0 & 0 & 0 & \boldsymbol{R} & 0 & 0 & 0 \\ 0 & 0 & 0 & 0 & [\boldsymbol{R}_{\mathsf{v}}]_\times & 0 & 0 \\ 0 & 0 & 0 & 0 & 0 & \boldsymbol{I}_{3\times 3} & 0 \\ \hdashline -\boldsymbol{R}^\top & 0 & 0 & 0 & [\widehat{\boldsymbol{p}}_t]_\times & 0 & 0 \\ 0 & -[\boldsymbol{R}_{\mathsf{v}}]_\times^\top & 0 & [\widehat{\boldsymbol{p}}_t]_\times & [\widehat{\boldsymbol{p}}_r]_\times & \boldsymbol{\mathcal{I}}_{p_f}^{\Omega} & 0 \\ 0 & 0 & -\boldsymbol{I}_{3\times 3} & 0 & -(\boldsymbol{\mathcal{I}}_{p_f}^{\Omega})^* & 0 & \mathrm{Div} \\ 0 & 0 & 0 & 0 & 0 & \mathrm{Grad} & 0 \end{array}\right]}_{\mathcal{J}} \underbrace{\begin{bmatrix} \partial_{\boldsymbol{r}_P} H \\ \partial_{\boldsymbol{R}_{\mathsf{v}}} H \\ \delta_{\boldsymbol{u}_f} H \\ \hdashline \boldsymbol{v}_P \\ \boldsymbol{\omega}_P \\ \boldsymbol{v}_f \\ \boldsymbol{\Sigma} \end{bmatrix}}_{\boldsymbol{z}}.
$$

Floating body as a pHDAE system

Final pHDAE system

This system fits into the framework detailed in Morandin 2019[19] and extends it.

$$
\begin{aligned}
\mathcal{E}(\boldsymbol{e})\partial_t \boldsymbol{e} &= \mathcal{J}(\boldsymbol{e})\boldsymbol{z}(\boldsymbol{e}) + \mathcal{B}_r(\boldsymbol{e})\boldsymbol{u}_\partial, \\
\boldsymbol{y}_r &= \mathcal{B}_r^*(\boldsymbol{e})\boldsymbol{z}(\boldsymbol{e}), \\
\boldsymbol{u}_\partial &= \mathcal{B}_\partial \boldsymbol{z}(\boldsymbol{e}) = \boldsymbol{\Sigma}\cdot\boldsymbol{n}|_{\partial\Omega} = \boldsymbol{\tau}|_{\partial\Omega}, \\
\boldsymbol{y}_\partial &= \mathcal{C}_\partial \boldsymbol{z}(\boldsymbol{e}) = \boldsymbol{v}_f|_{\partial\Omega},
\end{aligned}
$$

with $\boldsymbol{y}_r = (\boldsymbol{v}_P + [\boldsymbol{x}+\boldsymbol{u}_f]_\times^\top \boldsymbol{\omega}_P)|_{\partial\Omega}$.

Operator $\mathcal{E}$ is positive self-adjoint, $\mathcal{J}$ is formally skew-symmetric. The Hamiltonian satisfies

$$
\partial_{\boldsymbol{e}} H = \mathcal{E}^* \boldsymbol{z}.
$$

[19] V. Mehrmann and R. Morandin. "Structure-preserving discretization for port-Hamiltonian descriptor systems". In: *2019 IEEE 58th Conference on Decision and Control (CDC)*. 2019, pp. 6863–6868.

Power balance

The power balance equals the power due to the surface traction

$$
\begin{aligned}
\dot{H}(\boldsymbol{e}) &= \langle \partial_{\boldsymbol{e}} H, \partial_t \boldsymbol{e} \rangle_X, \\
&= \langle \boldsymbol{z}, \mathcal{E} \partial_t \boldsymbol{e} \rangle_X, \quad \text{Adjoint definition}, \\
&= \langle \boldsymbol{y}_\partial, \boldsymbol{u}_\partial \rangle_{\partial\Omega} + \langle \mathcal{B}_r^* \boldsymbol{z}, \boldsymbol{u}_\partial \rangle_{\partial\Omega}, \quad \text{I.B.P. on } \mathcal{J}, \\
&= \int_{\partial\Omega} \boldsymbol{u}_\partial \cdot (\boldsymbol{y}_\partial + \boldsymbol{y}_r) \, \mathrm{d}\Omega, \\
&= \int_{\partial\Omega} \boldsymbol{\tau} \cdot \boldsymbol{v} \, \mathrm{d}\Gamma,
\end{aligned}
$$

where $\boldsymbol{y}_\partial + \boldsymbol{y}_r := (\boldsymbol{v}_P + [\boldsymbol{\omega}_P]_\times (\boldsymbol{x} + \boldsymbol{u}_f) + \boldsymbol{v}_f)|_{\partial\Omega} = \boldsymbol{v}|_{\partial\Omega}$ is the velocity field at the boundary.

- Generic linear elastic model can be included (beams, plates etc.).
- Conservative forces are easily accounted for by introducing an appropriate potential energy. For example, the gravitational potential reads

$$H_{\text{pot}} = \int_\Omega \rho g \, {}^i r_z \, \mathrm{d}\Omega = \int_\Omega \rho g \left[{}^i r_{P,z} + \boldsymbol{R}_z (\boldsymbol{x} + \boldsymbol{u}_f) \right] \, \mathrm{d}\Omega.$$

- If case of vanishing deformations $\boldsymbol{u}_f \equiv 0$, the Newton-Euler equations on the Euclidean group $SE(3)$ are retrieved

$$\frac{d}{dt} \begin{pmatrix} {}^i\boldsymbol{r}_P \\ \boldsymbol{R}_{\text{v}} \\ \boldsymbol{p}_t \\ \boldsymbol{p}_r \end{pmatrix} = \begin{bmatrix} 0 & 0 & \boldsymbol{R} & 0 \\ 0 & 0 & 0 & [\boldsymbol{R}_{\text{v}}]_\times \\ -\boldsymbol{R}^\top & 0 & 0 & [\boldsymbol{p}_t]_\times \\ 0 & -[\boldsymbol{R}_{\text{v}}]_\times^\top & [\boldsymbol{p}_t]_\times & [\boldsymbol{p}_r]_\times \end{bmatrix} \begin{bmatrix} \partial_{\boldsymbol{r}_P} H \\ \partial_{\boldsymbol{R}_{\text{v}}} H \\ \partial_{\boldsymbol{p}_t} H \\ \partial_{\boldsymbol{p}_r} H \end{bmatrix}.$$

Outline

Discretized system

Same procedure but the integration by parts has to be applied to the Div operator to highlight the Neumann condition.

Finite-dimensional pHDAE system

After integration by parts of the Div operator

$$\begin{aligned}\mathbf{E}(\mathbf{e})\dot{\mathbf{e}} &= \mathbf{J}(\mathbf{e})\mathbf{z}(\mathbf{e}) + \mathbf{B}_\partial(\mathbf{e})\mathbf{u}_\partial, \\ \mathbf{M}_\partial \mathbf{y}_\partial &= \mathbf{B}_\partial^\top \mathbf{z}(\mathbf{e}).\end{aligned}$$

Dirichlet conditions

The set Γ_D for the Dirichlet condition has to be non empty, otherwise the deformation field is allowed for rigid movement, leading to a singular mass matrix: test and state shape functions must verify a homogeneous Dirichlet condition[20].

[20] O.P. Agrawal and A.A. Shabana. "Application of deformable-body mean axis to flexible multibody system dynamics". In: *Computer Methods in Applied Mechanics and Engineering* 56.2 (1986), pp. 217–245.

Outline

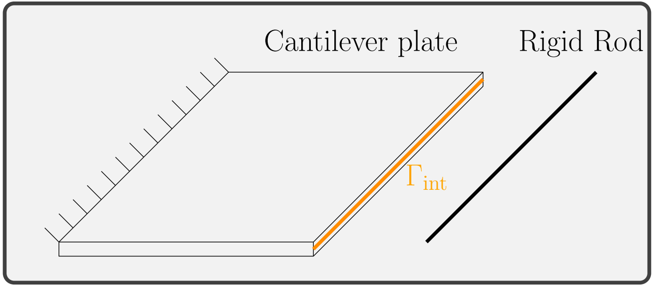
Cantilever plate
Rigid Rod
Γ_{int}

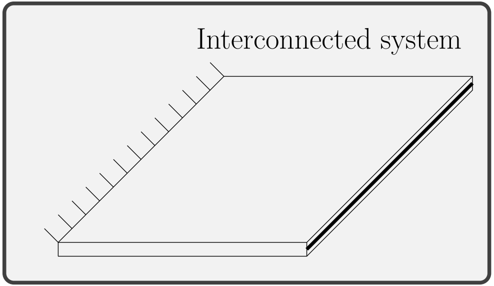
Interconnected system

Boundary Interconnection

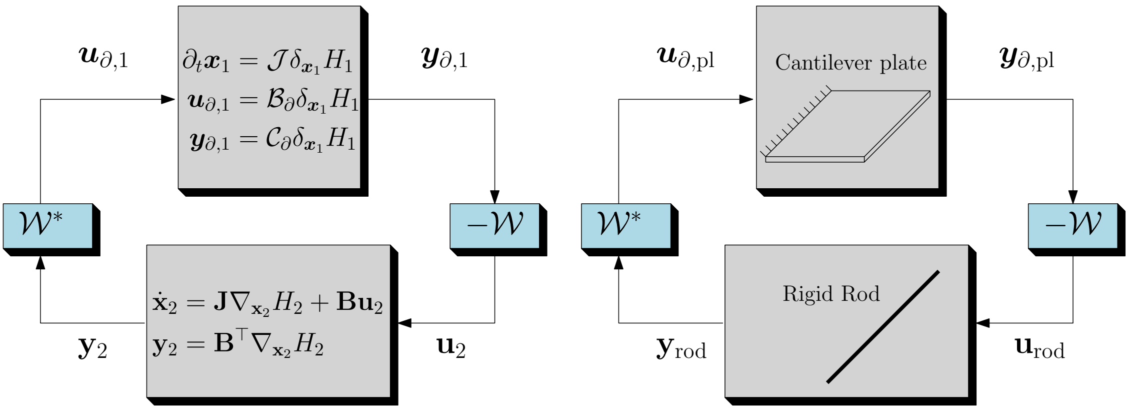

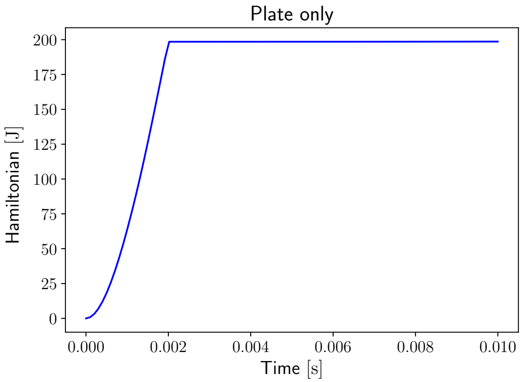
Plate only
Hamiltonian [J]
Time [s]
0
25
50
75
100
125
150
175
200
0.000
0.002
0.004
0.006
0.008
0.010

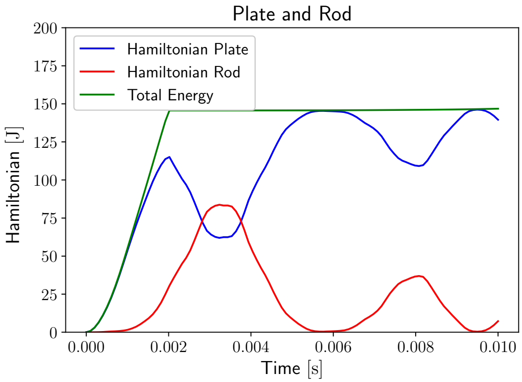
Plate and Rod
Hamiltonian Plate
Hamiltonian Rod
Total Energy
Hamiltonian [J]
Time [s]
0
25
50
75
100
125
150
175
200
0.000
0.002
0.004
0.006
0.008
0.010

Conclusion

Main contributions:

- A port-Hamiltonian formulation of elasticity, thermoelasticity and plate problems;
- Development and validation of a finite element based symplectic discretization characterized by an easy re-implementability;
- Floating frame based multibody dynamics: this multibody framework allows including the linear elastic models discussed in this thesis.

Outlook

Open problems and possible developments:

- Modelling: shell problems and non linear elasticity (ex. von Kármán plate);
- Discretization: efficient finite element for the Kirchhoff plate based on div-div conforming elements[21];
- Model reduction: application of POD methods, H_2-optimal strategies or Krilov subspace methods to the considered models;
- Multibody dynamics: computational aspect of the general quasi-linear problem (symplectic time-integration);
- Control: observer based strategies for boundary control[22] and reduced LQG design for distributed control[23].

[21] L. Chen and X. Huang. "Finite elements for divdiv-conforming symmetric tensors". In: *arXiv preprint arXiv:2005.01271* (2020).

[22] J. Toledo et al. "Observer-based boundary control of distributed port-Hamiltonian systems". In: *Automatica* 120 (2020).

[23] Y. Wu et al. "Reduced Order LQG Control Design for Infinite Dimensional Port Hamiltonian Systems". In: *IEEE Transactions on Automatic Control* (2020).

Journal articles

1. A. Brugnoli et al. “Port-Hamiltonian formulation and symplectic discretization of plate models. Part I: Mindlin model for thick plates”. In: *Applied Mathematical Modelling* 75 (2019). https://doi.org/10.1016/j.apm.2019.04.035, pp. 940 –960

2. A. Brugnoli et al. “Port-Hamiltonian formulation and symplectic discretization of plate models. Part II: Kirchhoff model for thin plates”. In: *Applied Mathematical Modelling* 75 (2019). https://doi.org/10.1016/j.apm.2019.04.036, pp. 961 –981

3. A. Brugnoli et al. “Port-Hamiltonian flexible multibody dynamics”. In: *Multibody System Dynamics* (2020). https://doi.org/10.1007/s11044-020-09758-6

4. A. Brugnoli et al. “Numerical approximation of port-Hamiltonian systems for hyperbolic or parabolic PDEs with boundary control”. In: *arXiv preprint arXiv:2007.08326* (2020). Under Review

International conferences with proceedings

1. A. Brugnoli et al. “Partitioned Finite Element Method for the Mindlin Plate as a Port-Hamiltonian system”. In: *IFAC-PapersOnLine* 52.2 (2019). 3rd IFAC Workshop on Control of Systems Governed by Partial Differential Equations CPDE 2019, pp. 88 –95
2. A. Brugnoli et al. “Interconnection of the Kirchhoff plate within the port-Hamiltonian framework”. In: *Proceedings of the 59th IEEE Conference on Decision and Control*. 2019
3. F.L. Cardoso-Ribeiro et al. “Port-Hamiltonian modeling, discretization and feedback control of a circular water tank”. In: *Proceedings of the 59th IEEE Conference on Decision and Control*. 2019
4. A. Brugnoli et al. “Partitioned Finite Element Method for Power-Preserving Structured Discretization with Mixed Boundary Conditions”. In: *Proceedings of the 21st IFAC World Congress*. Vol. 53. 2020, pp. 7647–7652
5. A. Brugnoli et al. “Structure-preserving discretization of port-Hamiltonian plate models”. Accepted for the 24st International Symposium on Mathematical Theory of Networks and Systems. 2021

Institut Supérieur de l'Aéronautique et de l'Espace

10 avenue Édouard Belin – BP 54032

31055 Toulouse Cedex 4 – France

Phone: +33 5 61 33 80 80

www.isae-supaero.fr

Institut Supérieur de l'Aéronautique et de l'Espace

SUPAERO